Chapter 3

Structural Effects caused by Inserting Small Hydrophilic Peptides into Multiple Sites on African Horse Sickness Virus Viral Protein 7.

3.1. Introduction

The purpose in constructing a VP7 protein with multiple cloning sites is for it to be able to accommodate and efficiently present multiple epitopes to the immune system. The advantage of a presenting epitopes at different positions would be that there is less attachment competition for immune reaction generation against these epitopes than there is against epitopes that are too closely located. As shown in chapter 2, the creation of VP7mt144/177/200 by the insertion of three multiple cloning sites, had an effect on the crystal formation abilities but did not totally destroy the protein's trimer formation abilities. To test the ability of VP7mt144/177/200 to accommodate epitopes at multiple sites and retain its structure, neutralising epitopes from AHSV serotype 4 Viral Protein 2 was utilised.

African horse sickness virus VP2 is one of the two proteins that constitute the outer layer of the virion, the other being VP5 (Roy *et al.*, 1994). This hydrophilic surface protein facilitates entry into mammalian cells during infection (Mertens *et al.*, 1996). Viral protein 2 proteins maintain strong structural similarities between serotypes but display the highest level of sequence variation of all the viral-encoded proteins (Fukusho *et al.*, 1987; Vreede and Huismans, 1994). The high variability and the hydrophilic nature displayed by certain regions of VP2, suggests that these regions are exposed to immunological pressure and may contain epitopes that are serotype specific (Venter *et al.*, 2000). It has also been shown that VP2 is the main determinant of serotype-discriminatory neutralising-specific immune response (Huismans *et al.*, 1987; Roy *et al.*, 1996; Scanlen *et al.*, 2002). Due to this, VP2 neutralising domains and epitopes has been a main subject of investigation.

The neutralising epitopes for AHSV VP2 serotype 4 were defined by Martínez-Torrecuadrada *et al.*, 2001. Two neutralising epitopes, 'a' (19 amino acids) and 'b' (24 amino acids), were identified between amino acid residues 321 - 339, and 377 - 400, respectively. It was shown that a combination of these two epitopes produced a much more effective neutralising response than the individualistic epitopes. The region also corresponds to the domain in which VP2 epitopes were identified on VP2 of

AHSV-3 by means of phage display libraries (Bentley *et al.*, 2000) and a region of importance identified on VP2 of AHSV-9 (Venter *et al.*, 2000). Based on this, it was decided to insert these two epitopes, 'a' at amino acid site 177 and 'b' at amino acid site 144. In total, three new constructs were synthesised; one containing the 'a' epitope, the other containing the 'b' epitope and the last construct containing both the epitopes at the given sites.

3.2. Materials and Methods

Materials

Reagents were obtained from the suppliers listed in section 2.2.

3.2.1. Annealing of Oligonucleotide Primers

The commercially synthesized oligonucleotide primers (Life Technologies) were resuspended in ddH_2O to a final concentration of 100 pmol/µl. Oligonucleotides for 'a' and 'b' were annealed in separate reactions consisting of the following: 200 pmol of each primer and 10x annealing buffer (100 nM Tris-HCl pH 7.5, 1 M NaCl, 10 mM EDTA) in a reaction volume of 10 /µl. The reaction mix was denatured at 92°C for 10 min followed by an annealing step at 65°C for one hour. Reactions were allowed to cool slowly at room temperature for one hour before being frozen away at -20°C until further use.

3.2.2. Cloning of Epitopes into the Modified VP7mt144/177/200 Construct and Expression of the Recombinant Proteins

Cloning of the 'a' and 'b' VP2 epitopes into pFastBac-VP7mt144/177/200 construct was achieved by methods described in chapter 2, with one variation. The ligation of the annealed oligonucleotides to the digested and purified pFastBAC-VP7mt144/177/200 proceeded at 16 °C for 16 h. A 10:1, ratio of insert: vector molecules was again applied in the ligation mixture.

Ligation was followed by transformation of the DNA into competent *E.coli* Xl1 Blue cells, which yielded colonies containing the recombinant plasmids. After DNA analyses of samples by electrophoretic separation on 4% agarose gels, the purified DNA of the two single epitope recombinant constructs were sequenced. The three recombinant pFastBac-containing-VP7-mutants were transformed into competent *E.coli* DH_{10}Bac™ cells where transposition of the relevant genes occurred

to form composite bacmid DNA for use during transfection and the creation of the recombinant viruses. Protein expression was analyzed on a 15% SDS-PAGE gels before solubility and sonication essays were conducted. The protein morphology of constructs were further analyzed and viewed under the S.E.M.

Table 3.1. Oligonucleotide sequence of the VP2 epitopes.

OLIGONUCLEOTIDE SEQUENCE
19 amino acid Epitope 'a'
VP27A4F 5' P-TAAGAAGAAAGAAGAGGGTGAGGATGATACTGCTCGACAGGAGATAAGAAAAGCATGGCTGCAGG 3' *Nsi*I K K K E E G E D D T A R Q E I R K A W *Pst*I *BssH*II
VP27A4R 5' P-CGCGCCTGCAGCCATGCTTTTCTTATCTCCTGTCGAGCAGTATCATCCTCACCCTCTTCTTTCTTCTTATGCA 3' *BssH*II *Pst*I *Nsi*I
24 amino acid Epitope 'b'
VP242BF 5' P-AATTCCTCGAGGTAGACGTTGATCCAAATAAGGGTAAGTGGAAAGAACATATAAAAGAGGTAACCGAAAAATTA EcoRI XhoI V D V D P N K G K W K E H I K E V T E K L AAGAAAGCGG 3' K K A SalI
VP242BR 5' P-TCGACCGCTTTCAATAATTTTTCGGTTACCTCTTTTATATGTTCTTTCCACTTACCCTTATTTGGATCAACGTCTAC SalI CTCGAGG 3' XhoI EcoRI

3.3. Results

3.3.1. Epitope Insertion

The complimentary oligonucleotides for the neutralising epitopes of AHSV VP2 serotype 4, 'a' (19 aa) and 'b' (24 aa), were annealed and inserted respectively into amino acid site 177 and 144 of the pFastBac-VP7mt144/177/200 plasmid vector, creating VP7mt144/177-A/200 and VP7mt144-B/177/200. The recombinant construct containing the 'b' epitope at the 144 amino acid site, again underwent the cloning process as described above, this time inserting the 'a' epitope at the 177 amino acid site, creating VP7mt144-B/177-A/200 (Fig. 3.1.). The forward oligonucleotide sequence (Table 3.1.) for the 'a' epitope (VP27A4F) included a 5'-T overhang, whereas the complementary reverse oligonucleotide sequence (VP27A4R) contained a 3'-ATGCA overhang. These regions code for a digested *Nsi*I restriction endonuclease site, an isoschizomere of *Pst*I, meant to destroy the *Pst*I site of pFastBac-VP7mt144/177/200. Also included in these complementary oligonucleotide sequences for the 'a' epitope, was a new PstI endonuclease site next to a 3' overhang coding for *BssHII*, which binds to the *BssHII* digested pFastBac-VP7mt144/177/200. The oligonucleotide sequences for the 'b' epitope has the same type of overhangs, including 3' nucleotides for *Sal*I, an isoschizomere of *Xho*I, and an additional *Xho*I next to an overhang for EcoRI at the 5' end of forward of the sequence.

3.3.2. Nucleotide Sequence Determination and Hydropathy Predictions

The primers listed in table 2.1. were used during automated DNA sequencing (section 2.2.10) to determine the nucleotide sequence of the newly constructed VP7mt144/177-A/200, VP7mt144-B/177/200 and VP7mt144-B/177-A/200. The complete sequences, which confirmed the presence of the inserted epitopes into the constructs, were attained from overlapping sequences.

Nucleotide sequence determination did indicate two mutations in both the VP7mt144-B/177/200 (Appendix B-2) and VP7mt144-B/177-A/200 (Appendix B-3) constructs. The same two new mutations are present in both these constructs. This is probably due to the fact that VP7mt144-B/177/200 was used to create VP7mt144-B/177-A/200. At nucleotide position 514 and 515, two adenosines were substituted with two thymidines. This mutation occurs in the oligonucleotide sequence for the 'b' epitope and initially occurred in the synthesized oligonucleotide. Both of these changes occur in one codon, substituting a lysine for a leucine. This creates a drop in the

hydrophilicity value at this amino acid position from +3.0 to -1.8, according to the Hopp and Woods predictive method (Hopp and Woods, 1981; Hopp and Woods, 1983). This small change in hydrophylicity could possibly have drastic effects on the stability of the structure, although, at this stage, it was unsure. It would also have had an effect on the generated immune response, if these constructs were to be used for immune binding studies.

Sequence comparisons and alignments were done using ClustalX version 1.81 (Higgins and Sharp, 1988; Higgins *et al.*, 1996) (Appendix B). Subsequent hydropathy analyses of the total recombinant structures were done (Fig. 3.2.) using the Hopp and Woods predictive method (Hopp and Woods, 1981; Hopp and Woods, 1983) from the ANTHEPROT package (Geourjon *et al.*, 1991; Geourjon and Deleage, 1995).

Table 3.2. Hydrophilic characters the AHSV-4 epitopes (Hopp and Woods, 1981; Hopp and Woods, 1983).

Insert	**Amino Acid Amount**	**Hydrophilic Character of Insert**	
		Total	**Average**
Epitope 'a'	19	+158	+8.3
Epitope 'b'	24	+131	+5.5

As can be seen in table 3.2 and figure 3.2., both the epitopes are extremely hydrophilic. This is expected since, being presented on the surface of the AHSV particles, the are both in direct contact with the hydrophilic infected environment. The shorter nineteen amino acid 'a' epitope, with a hydrophilic character of +158, is far more hydrophilic than the twenty-four amino acid 'b' epitope, which only has a hydrophilic total of +131. The effect of these extreme hydrophilic insertions on the structure of VP7mt144/177/200 could at this stage not be predicted.

3.3.3. Baculovirus Expression

The Bac-to-Bac™ expression system was used to express the three recombinant pFastBac constructs. *E.coli* DH_{10}Bac™ cells were transformed with the pFastBac transfer vectors containing the constructs, where transposition of the recombinant VP7 genes occurred into the baculovirus genomes (2.2.13) Recombinant baculovirus genomes were selected for and the DNA isolated (2.2.14) before being transfected into Sf9 insect cells (2.2.15). The newly generated recombinant baculoviruses were then used in subsequent infections before protein expression analyses by SDS-PAGE gel electrophoresis (2.2.17)

The gel analysis (Fig. 3.3.) confirmed the expression of VP7mt144/177-A/200 (41 kDa), VP7mt144-B/177/200 (42 kDa) and VP7mt144-B/177-A/200 (44 kDa). VP7mt144/177-A/200 and VP7mt144-B/177-A/200 have much lower protein expression levels than VP7mt144/177/200 and VP7mt144-B/177/200. The 41 kDa VP7mt144/177-A/200 seems to have a much slower electrophoretic mobility rate than the 42 kDa VP7mt144-B/177/200, causing it to appear higher on the SDS-PAGE gel analysis. Another interesting phenomenon is that all three the new recombinants form double protein bands.

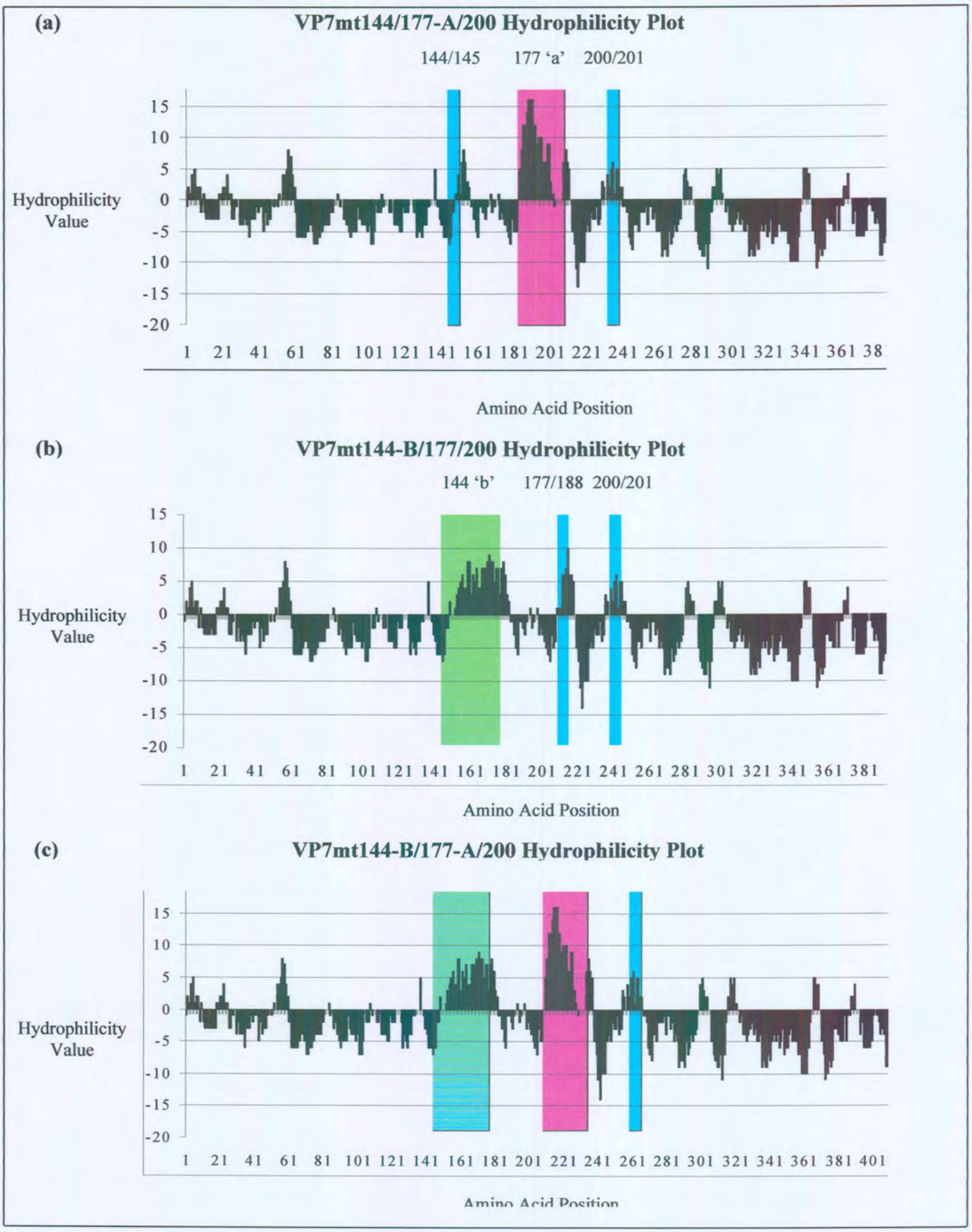

Figure 3.2. Hydrophilicity Plots of (a) VP7mt144/177-A/200, (b) VP7mt144-B/177/200 and (c) VP7mt144-B/177-A/200 according to the Hopp and Woods Predictive method (Hopp and Woods, 1981; Hopp and Woods, 1983)

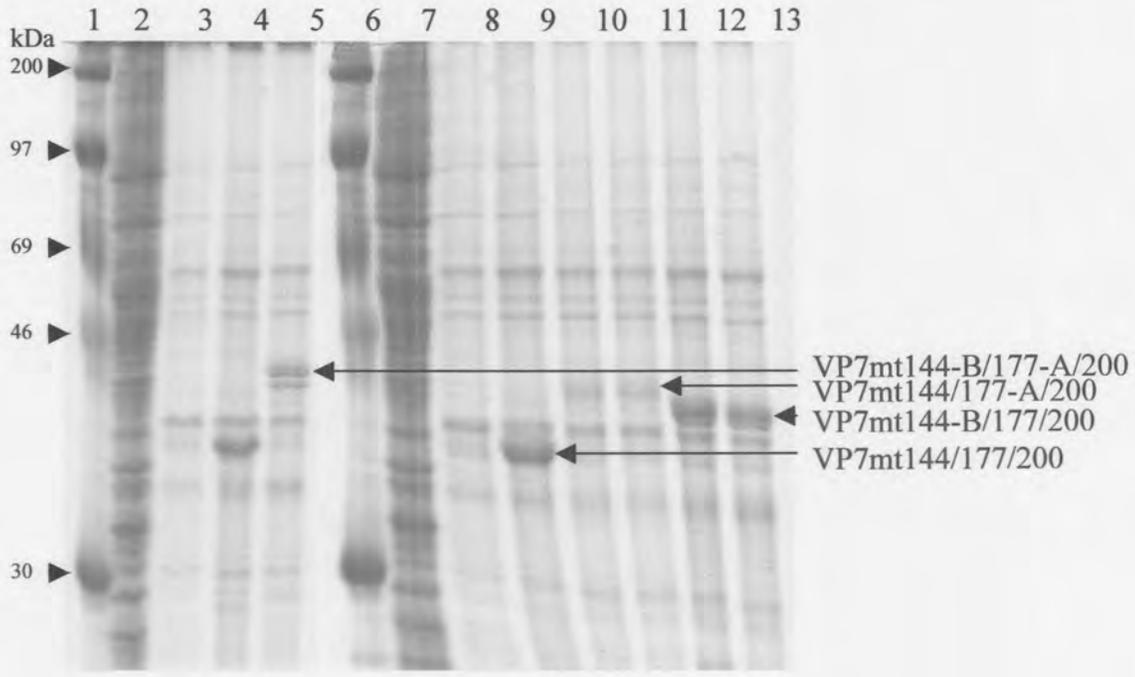

Figure 3.3. Analysis of the newly created epitope mutants compared to VP7mt144/177/200 on a 15% SDS-PAGE gel. Lanes 1 and 6 represent the protein size marker. Lanes 2 and 7 contain proteins from a mock infection, whereas lanes 3 and 8 contain wild-type baculovirus-infected cells lysates. Lanes 4 and 9 contain expressed VP7mt144/177/200 (39 kDa). Lane 5 contains the 44 kDa VP7mt144-B/177-A/200 protein. Lanes 10 and 11 contain the 41 kDa VP7mt144/177-A/200 protein, whereas lanes 12 and 13 contain the expressed VP7mt144-B/177/200 protein (42 kDa).

3.3.4. Purification of Recombinant VP7 Particles on Sucrose Gradients

Changes in solubility and stability that might have been caused by the insertion of the two epitopes at amino acid position 144 and 177 of VP7mt144/177/200 were studied. VP7mt144/177-A/200, VP7mt144-B/177/200 and VP7mt144-B/177-A/200 were expressed in Sf9 cells by recombinant baculoviruses containing the respective genes. Cells were lysed 72 h post-infection, and the

recombinant VP7 proteins were harvested and purified by rate zonal centrifugation on 50%-70% discontinuous sucrose gradients. SDS-PAGE gels were used to analyse the proteins in the fractions of the sucrose gradients and the intensities were quantified using Sigma Gel™ software program (Jandel Scientific). VP7mt144/177/200 was used as a standard control during all of these studies. Sonication studies were also done, for not only is it a method to remove protein aggregation, but it also serves as another stability study when compared to control sonicated VP7mt144/177/200.

Figure 3.4. depicts the comparative protein particle distribution of VP7mt144/177-A/200. Of the unsonicated VP7mt144/177-A/200 particulate distribution (Fig. 3.4.a), 83% of the protein occurs in the pellet of the gradient. This is 28% more than the percentage of VP7mt144/177/200 proteins in the pellet. The large particulate VP7mt144/177-A/200 structures in the first three fractions, yield approximately the same amount of proteins as the small particulate structures found in the last three fractions (7.6%). This is in contradiction with VP7mt144/177/200 where all the structures formed by VP7mt144/177/200 and not aggregated in the pellet, are large and occur in the bottom fractions of the sucrose gradients. The VP7mt144/177/200 construct forms no small particulate structures, which might be free soluble trimers, in the last fraction like VP7mt144/177-A/200. The sonicated products of the two constructs resemble each other except that VP7mt144/177-A/200 seems to form a more defined size structure after sonication than VP7mt144/177/200, as is indicated by the peak in the third fraction.

VP7mt144-B/177/200, which is longer yet less hydrophilic than VP7mt144/177-A/200, seems to be more soluble than with far less aggregation when compared to VP7mt144/177/200 (Fig. 3.5.). Only 17% of this protein occur in the pellet of the gradient. Most of the proteins for this construct (52%) occur in the first four fractions of the gradient, whereas the same fractions for VP7mt144/177/200 contain only 36.4% of the total amount. VP7mt144-B/177/200 also has a higher amount of small particles in the last four soluble fractions of the gradient (19.1%). The sonication product resembles that of VP7mt144/177-A/200 with the same, but higher, distinct peak in the third fraction from the bottom of the gradient. This is indicative of a size formation preference displayed by the construct for smaller particulate structures with a roughly constant size.

The simultaneous effect of inserting both the epitopes into VP7mt144/177/200 can be seen when analyzing the solubility of VP7mt144-B/177-A/200 (Fig. 3.6.). The protein particulate distribution of unsonicated VP7mt144-B/177-A/200 closely resembles that of VP7mt144/177/200. The pellet containing the aggregated proteins as well as the insoluble bottom fractions contain approximately the

same protein levels. The particulate protein distribution of VP7mt144-B/177-A/200, however, contains 5% small particles in the last three soluble fractions compared to only 1% as formed by VP7mt144/177/200. Sonication of the VP7mt144-B/177-A/200 results in the same protein particle distribution as VP7mt144/177-A/200 and VP7mt144-B/177/200.

3.3.6. Scanning Electron Microscopy (S.E.M.)

The second, third and fourth fractions of the protein samples were pooled and prepared for S.E.M study. The same structures as formed by VP7mt144/177/200 (Fig 2.13.c and d) are also being formed by VP7mt144/177-A/200 (Fig. 3.7.a. and b.), VP7mt144-B/177/200 (Fig. 3.7.c. and d.) and VP7mt144-B/177-A/200 (Fig. 3.7.e. and f.). Most of the structures have approximately the same size with a rough, flat and almost circular appearance. Web-like tentacles/ cables can also be observed where clusters of particulate structures occur on the grid (Fig. 3.7.d. and f.).

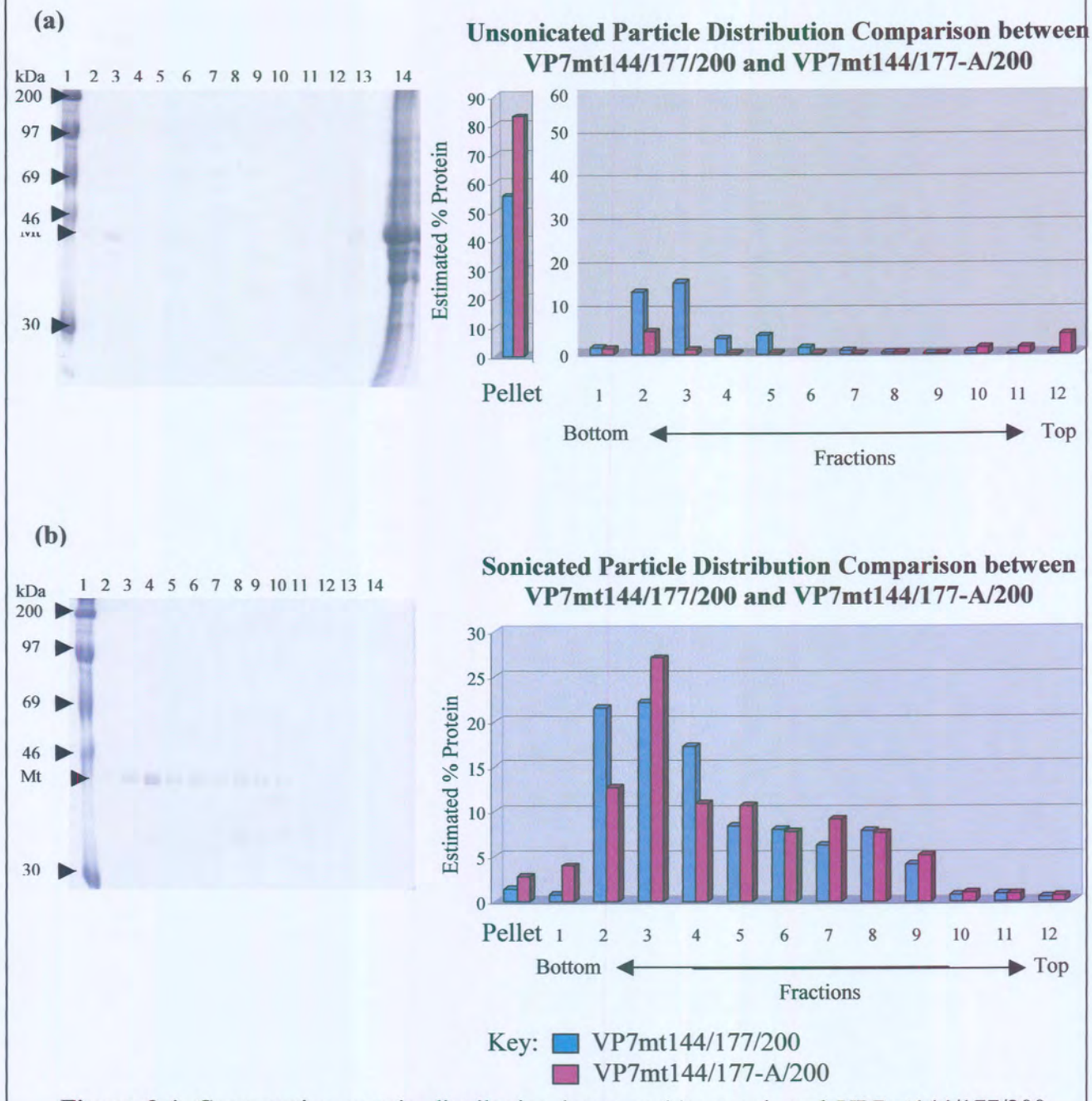

Figure 3.4. Comparative protein distribution between (a) unsonicated VP7mt144/177/200 and VP7mt144/177-A/200. (b) Represents a comparative protein distribution between 25 pulse sonicated pellets of VP7mt144/177/200 and VP7mt144/177-A/200. A Sorvall AH-650 rotor was used at 12000 rpm for 75 min at 4°C to centrifuge the proteins on a 50%-70% sucrose gradient. SDS-PAGE electrophoresis was used to analyze the collected fractions and quantification of the fractional distribution was done using the Sigma Gel™ analysis program. On the SDS-PAGE gels, lane 1 contains the protein size marker, whereas lanes 2-13 contain the fractions as collected from the bottom to the top of the gradients. Lane 14 represents the protein pellet of the gradient.

(a)

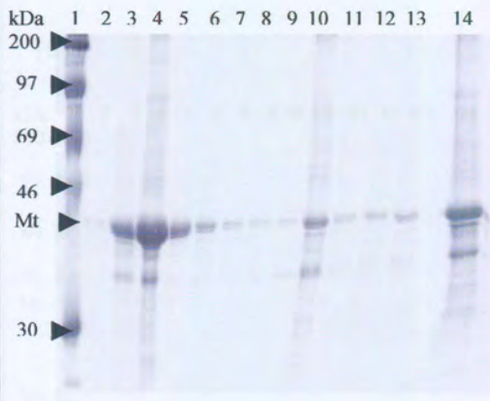

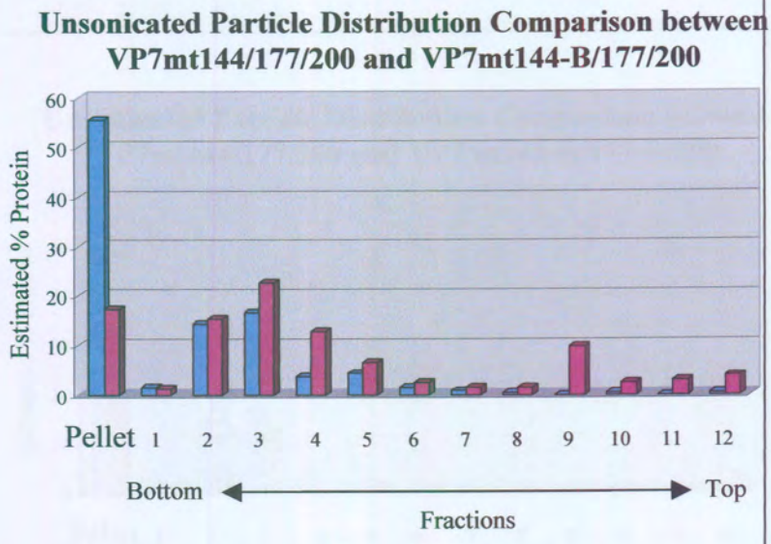

(b)

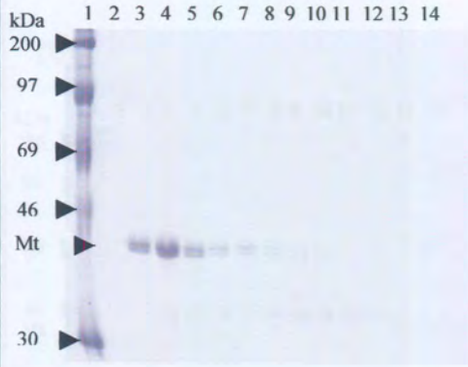

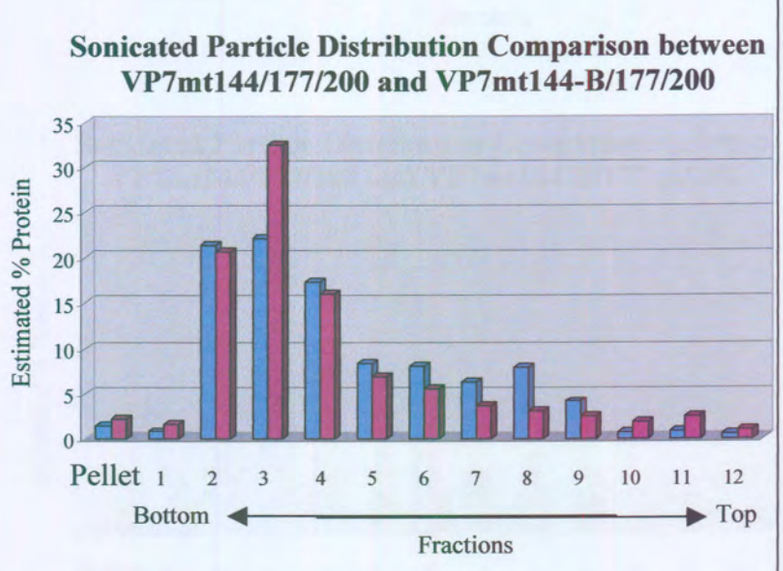

Figure 3.5. Comparative protein distribution between (a) unsonicated VP7mt144/177/200 and VP7mt144/177-B/200. (b) Represents a comparative protein distribution between 25 pulse sonicated pellets of VP7mt144/177/200 and VP7mt144/177-B/200. Centrifugation of the proteins proceeded on a 50%-70% sucrose gradient using a Sorvall AH-650 rotor at 12000 rpm for 75 min at 4°C. This was followed by SDS-PAGE electrophoresis analyses, quantification by the Sigma Gel™ analysis program and conversion to the shown graphic form. Lane 1 on the SDS-PAGE gel contains the protein size marker, whereas lanes 2-13 contain the fractions as collected from the bottom to the top of the gradients. Lane 14 represents the protein pellet of the gradient.

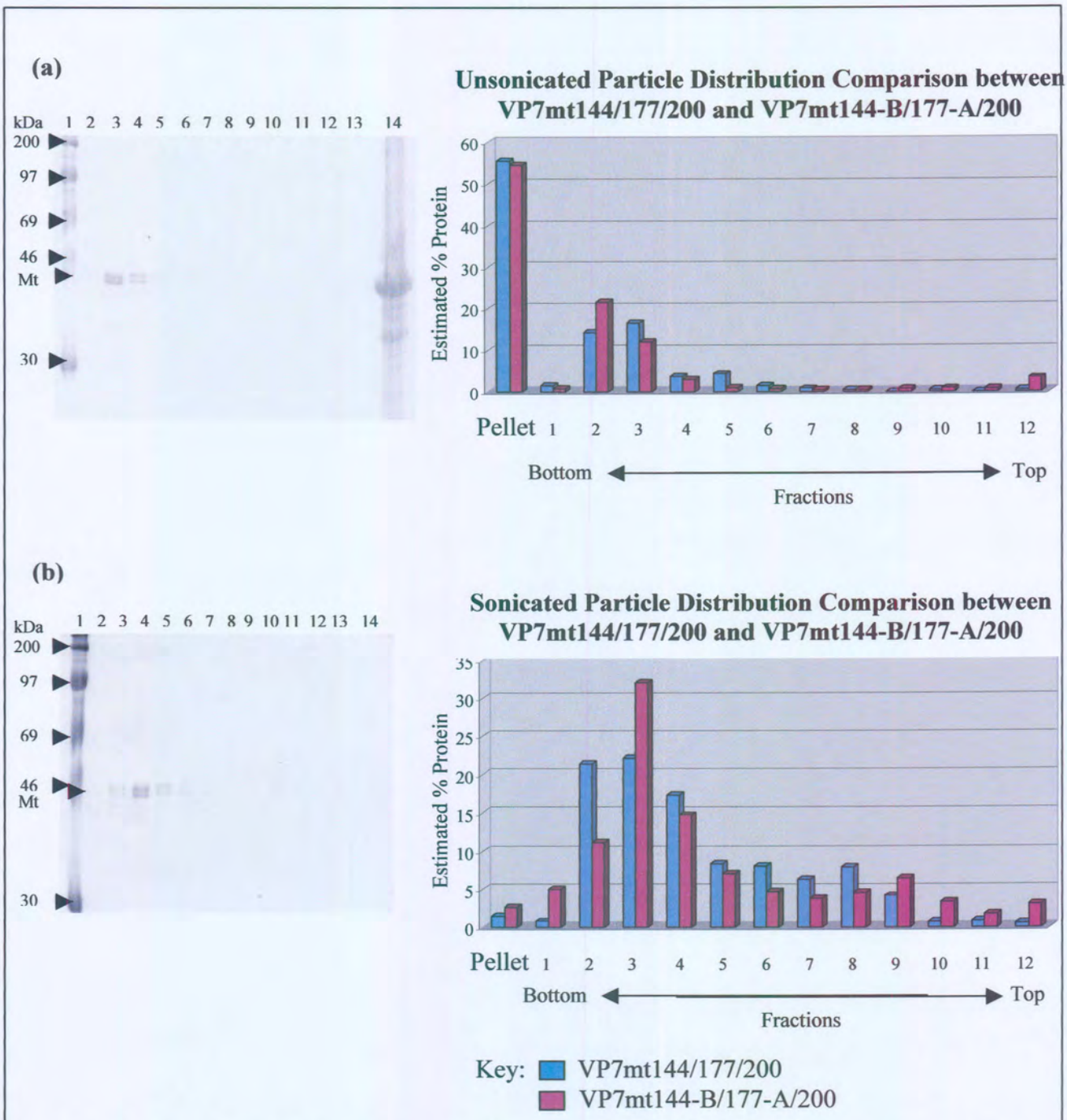

Figure 3.6. Comparison of protein fractional distribution between (a) unsonicated VP7mt144/177/200 and VP7mt144-B/177-A/200 and (b) 25 pulse sonicated pellets of VP7mt144/177/200 and VP7mt144-B/177-A/200. Proteins were centrifuged on a 50%-70% sucrose gradient using a Sorvall AH-650 rotor at 12000 rpm for 75 min at 4°C, analyzed by SDS-PAGE electrophoresis, quantified by the Sigma Gel™ analysis program and converted to the shown graphic form. On the SDS-PAGE gels, lane 1 contains the protein size marker. Lanes 2-13 contain the fractions as collected from the bottom to the top of the gradients, whereas lane 14 represents the protein pellet of the gradient.

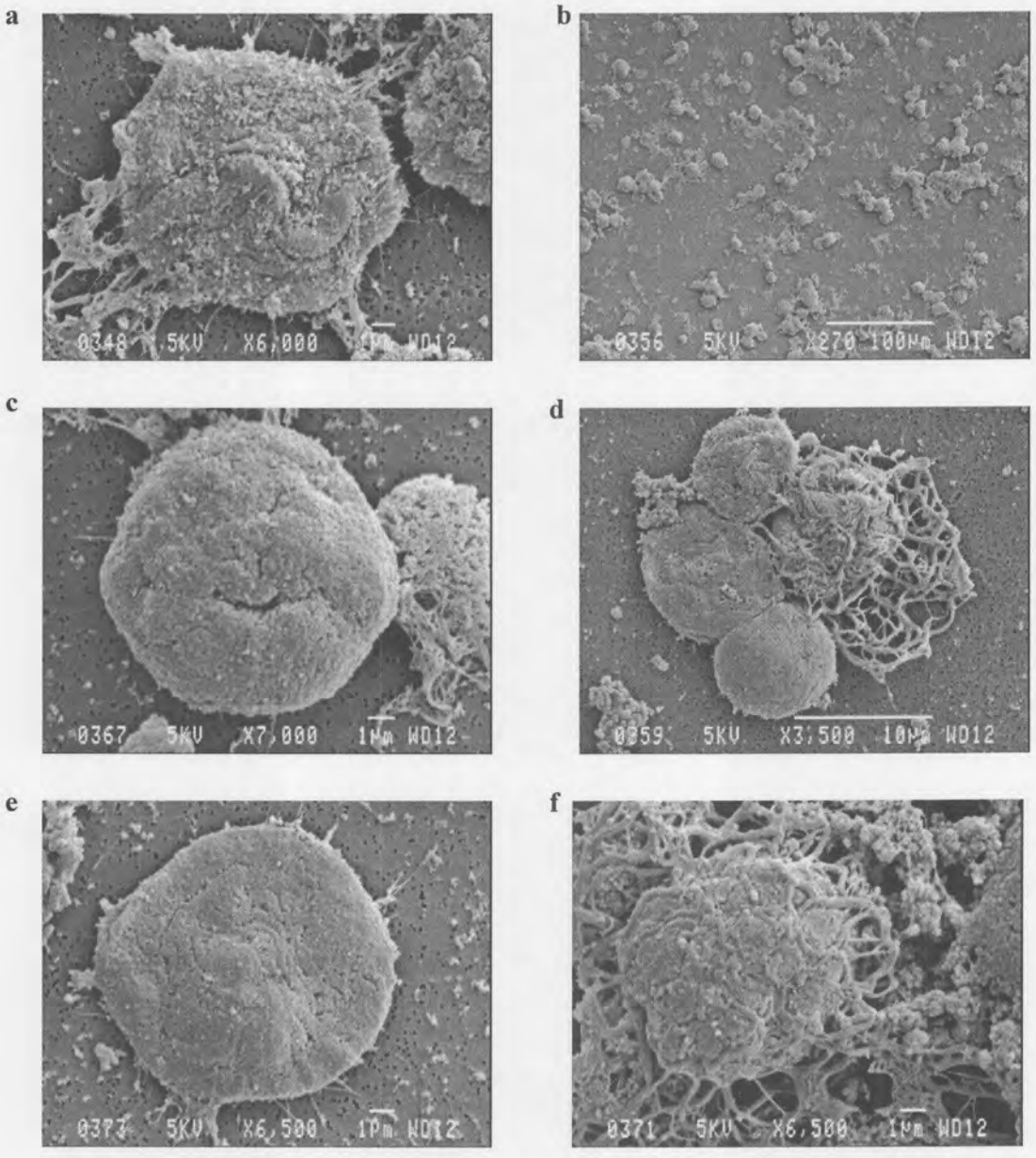

Figure 3.7. Scanning Electron Microscopy photographs depicting the structures formed by the different protein constructs: (a) VP7mt144/177-A/200 and a wide-angle view in (b). (c) Depicts VP7mt144-B/177/200 with a wide-angle view in (d). (e) And (f) are structures formed by VP7mt144-B/177-A/200.

3.4. Discussion

The possibility to efficiently present different epitope-containing peptides at multiple sites on a single subunit vaccine has definite advantages. The major advantage being that each epitope is individually presented to the immune system without the inhibition that another epitope, located next to the first, might cause. It also presents the possibility of presenting different peptides that could provide protection against different diseases or different serotypes of the same virus on a single subunit vaccine. As can be seen in chapter two, the insertion of three multiple cloning sites into VP7 resulted in morphological changes on the crystal structures formed by VP7. The insertion of twenty-two amino acids into modified VP7 containing only a single multiple cloning site at amino acid position 177 had almost no morphological effects on the crystal structures formed by VP7 (Meyer, 2002). This prompted a study into the effect of inserting larger regions into at least two of the three multiple cloning sites in VP7mt44/177/200.

The two neutralising epitopes of AHSV-4 VP2, 'a' and 'b', were chosen for insertion at amino acid site 177 and 144 respectively. The nineteen amino acid 'a' epitope is more hydrophilic than the twenty-four amino acid 'b' epitope (Table 3.2), the effect of which could not be determined until after solubility studies were conducted. The two constructs with the single epitope insertions, VP7mt144/177-A/200 and VP7mt144-B/177/200, not only served as controls for the double construct, VP7mt144-B/177-A/200. They also functioned as studies into the effects caused by larger amino acid single insertions into VP7mt144/177/200 at the two respective multiple cloning sites.

The insertion of the hydrophilic 'a' epitope at position 177 of VP7mt144/177/200 had a definite change on the solubility of the structure (Fig. 3.4.). There was a large increase in aggregation of the assembled protein units and an increase in the smaller particles, possibly free soluble trimers. This is possibly due to the tearing open of the close-knit hydrophobic structural units by the hydrophilic insertions. More hydrophobic regions are exposed to the surface of a structural unit, causing the units to aggregate. The increase in free trimers could be a direct effect of the increase in solubility by the addition of the extremely hydrophilic 'a' epitope.

The insertion of the 'b' epitope into position 144 of VP7mt144/177/200 to create VP7mt144-B/177/200 lowered the aggregation of the structural units normally formed by VP7mt144/177/200

(Fig. 3.5.). The effect on the overall structure an insert has is not only dependent on the characteristics of the insert but also the position the insertion is made. The effect that this twenty-four amino acid hydrophilic insert had on the structure of VP7mt144/177/200 might be because of both the insert position and the characteristics of the insert. The aggregational tendency of the units was lowered probably because of a tightening of the structure around possible hydrophobic regions. The insert also increased the overall hydrophilicity of the protein unit, as can be seen in the decrease in aggregation and the greater amounts of smaller particles that occur in the top of the sucrose gradients

The construct containing both the epitopes, VP7mt144-B/177-A/200, has an intermediate aggregational tendency of the particle structures when compared to the two previously discussed constructs (Fig. 3.6.). The structural effect caused by the insertion of the 'a' epitope at site 177 of VP7mt144/177/200 is neutralised by the insertion of the 'b' epitope at the 144 amino acid site. This results in VP7mt144-B/177-A/200's solubility being almost the same as the protein fractional distribution of VP7mt144/177/200. The insertion of the peptides resulted in a reduction in the size of the particles as seen by the increase in small particles found at in the top fractions of the gradients.

As can be seen from the sonication studies, the structural units can be freed from the aggregation resulting in units with a distinct size. The administered sonication pulses were not enough to reduce the structures to free trimers in the soluble fractions of the gradient. The electron microscopy studies (Fig. 3.7.) supported the evidence pointing to retention of the structure formed by VP7mt144/177/200, by all three the new constructs.

Chapter 4

The Effect of Various Lengths of Viral Protein 2 of African Horse Sickness Virus on Modified Viral Protein 7.

4.1. Introduction

The major disadvantage of virus like particles as antigen carriers, is the limitation in the size of the peptides that can be inserted. In order to utilise the full potential of the VP7 particles effectively as an antigen presentation system; the structure must be able to accommodate large epitope-containing insertions. As shown in chapter 2, the insertion of three multiple cloning sites in VP7mt144/177/200 had an effect on the morphology and appearance of the VP7 crystalline particles but it did not appear to prevent the protein from assembling into particles that could be purified on sucrose gradients. These findings were the same for the small peptides that were inserted into the 144 and 177 amino acid sites of VP7mt144/177/200. It is therefore assumed that the proteins' ability to assemble into trimers have not been destroyed in any of the cases. To further investigate the ability of VP7 to accommodate the insertion of a large range of hydrophilic amino acid peptides we inserted a range of peptides of diffirent sizes in amino acid site 177 of the vector. These peptides overlapped the previously characterised neutralising epitopes on major outer capsid protein VP2 of AHSV serotype 4. The nature of VP2 neutralising domains and epitopes makes it a suitable candidate for investigating the ability of VP7 to accommodate a range of hydrophilic peptides of various sizes.

It is also important to construct a range of different sequence inserts since it has been found that subunit vaccines are dependant on the characteristics of the insert. In other words, the subunit vaccines could retain structure with large inserts but would lose structure with a much smaller but different insert. This was best illustrated by the research done on non-structural protein 1 (NS1) of BTV. This protein, which forms tubules when expressed in insect cells, has been investigated as a possible subunit epitope presentation vaccine. Extension mutants of foreign antigenic sequences involving up to 16 amino acids added to the C terminus of NS1 were shown to form tubules, although an extension of 19 amino acids inhibited tubule formation (Monastryrskaya *et al.*, 1995). Later it was found that the 64 kDa NS1 was still able to form the tubules even after being fused to a green fluorescent protein with an approximate size of 31 kDa (Ghosh *et al.*, 2002).

4.2. Materials and Methods

Materials

Dr. M van Niekerk provided the TOPO vector containing AHSV-4 VP2. Other reagents were obtained from the suppliers described in section 2.2.

4.2.1. Polymerase Chain Reaction

Polymerase chain reaction was used to amplify the VP2 fragments from the obtained VP2-containing TOPO vector. Primers, containing the necessary attached restriction endonuclease sites (Table 4.1), were designed to anneal at specific position on the VP2 template, which would produce the required lengths of amplified fragments. All PCR reactions were carried out using reagents described in section 2.2.1

The amplification conditions for all four reactions were as follows: 1 cycle at 94°C for 2 min; 25 cycles 93°C for 45 sec, 62°C for 1 min, 72°C for 2 min; 1 cycle at 72°C for 10 min.

Table 4.1. Primer sequences used in PCR of the VP2 fragments.

PRIMER NAME	DIRECTED POSITION	OLIGONUCLEOTIDE SEQUENCE	Tm °C
Different Forward Primers			
VP100F	Nucleotides 931-960	5' CACCTGCAGTTTGATTTTTTGACAACATTCGTTCATGCG 3' *Pst*I	59
VP150F	Nucleotides 781-814	5' CACCTGCAGAAAGGTCCACTGAATGACTTACGAGTTAAAATTG 3' *Pst*I	61
VP200F	Nucleotides 631-660	5' CACCTGCAGAAGCTGAGATTTGGAATGATGTACCCACAC 3' *Pst*I	63
VP250F	Nucleotides 481-510	5' CACCTGCAGGAGAGTAAGAGAAAAGCAATCCTTGATCAG 3' *Pst*I	62
Single Reverse Primer			

VP2EPIR	Nucleotides 1206-1230	5' GTTGCGCGCTTGGCATGGTTGTCCTCCATTTTCG 3' *BssH*II	63

4.2.2. Cloning of VP2 Regions into the Modified VP7mt144/177/200 Construct and Expression of the Recombinant Proteins

Cloning of the VP2 amplified fragments into pFastBac-VP7mt144/177/200 construct was achieved by methods described in chapter 2, with one variation. The ligation of the separate fragments to the digested and purified pFastBAC-VP7mt144/177/200 proceeded at 16 °C for 16 h. A 3:1, ratio of insert: vector molecules was used in the ligation mixture.

Subsequent transformation yielded colonies containing the recombinant plasmids. DNA samples were analyzed by the electrophoretic separation of DNA on 4% agarose gels. The purified DNA of the four recombinant constructs was sequenced before being used in a transposition reaction to form composite bacmid DNA for use during transfection and the creation of the recombinant viruses. Protein expression was analyzed on a 15% SDS-PAGE gels before solubility and sonication essays were conducted. The protein morphology of constructs were further analyzed and viewed under the S.E.M.

4.3. Results

The TOPO vector containing VP2 of AHSV-4, as provided by Dr. M van Niekerk, served as template for the amplification of the four inserts. All of these inserts, the 100 aa, 150 aa, 200 aa and the 250 aa amplified regions, contained both the neutralising epitopes for AHSV VP2 serotype 4. It was thought that any effect such large inserts might have on the structure of the VP7mt144/177/200 construct, would be more subdued if the inserts were cloned into the centrally located 177 amino acid site. This multiple cloning site was constructed in the middle of a highly flexible RGD containing loop. Also, further support for this choice came from the research conducted by Meyer, 2002, as mentioned in section 2.4., which showed that AHSV VP7 was still able to form crystals when a twenty-two amonio acid insert had been made at amino acid position 177.

4.3.1. Synthesis of the Size-Constructs

The cloning procedure of the four inserts is outlined in figures 4.1 and 4.2 and were all individualistically done in one step. The primers (Table 4.1.) used for the amplification of the four fragments added a 5' *Pst*I restriction enzyme site and a 3' *Bss*HII site to the fragments. The four obtained PCR products, 318 bp, 468 bp, 618 bp and 768 bp, were subjected to a double separate digestion with the *Pst*I and *Bss*HII restriction endonucleases and purified via the High Pure™ PCR Product Purification Kit (Roche Diagnostics). The fragments were then separately cloned into the *Pst*I and *Bss*HII sites of the digested and cleaned pFastBac-VP7mt144/177/200 plasmid vector. This gave rise to four new constructs: VP7mt144/177-100/200, VP7mt144/177-150/200, VP7mt144/177-200/200, VP7mt144/177-250/200. The four constructs were digested with *Eco*RI and *Xba*I (Fig. 4.3.) to confirm the insertion of the fragments before nucleotide sequence determination.

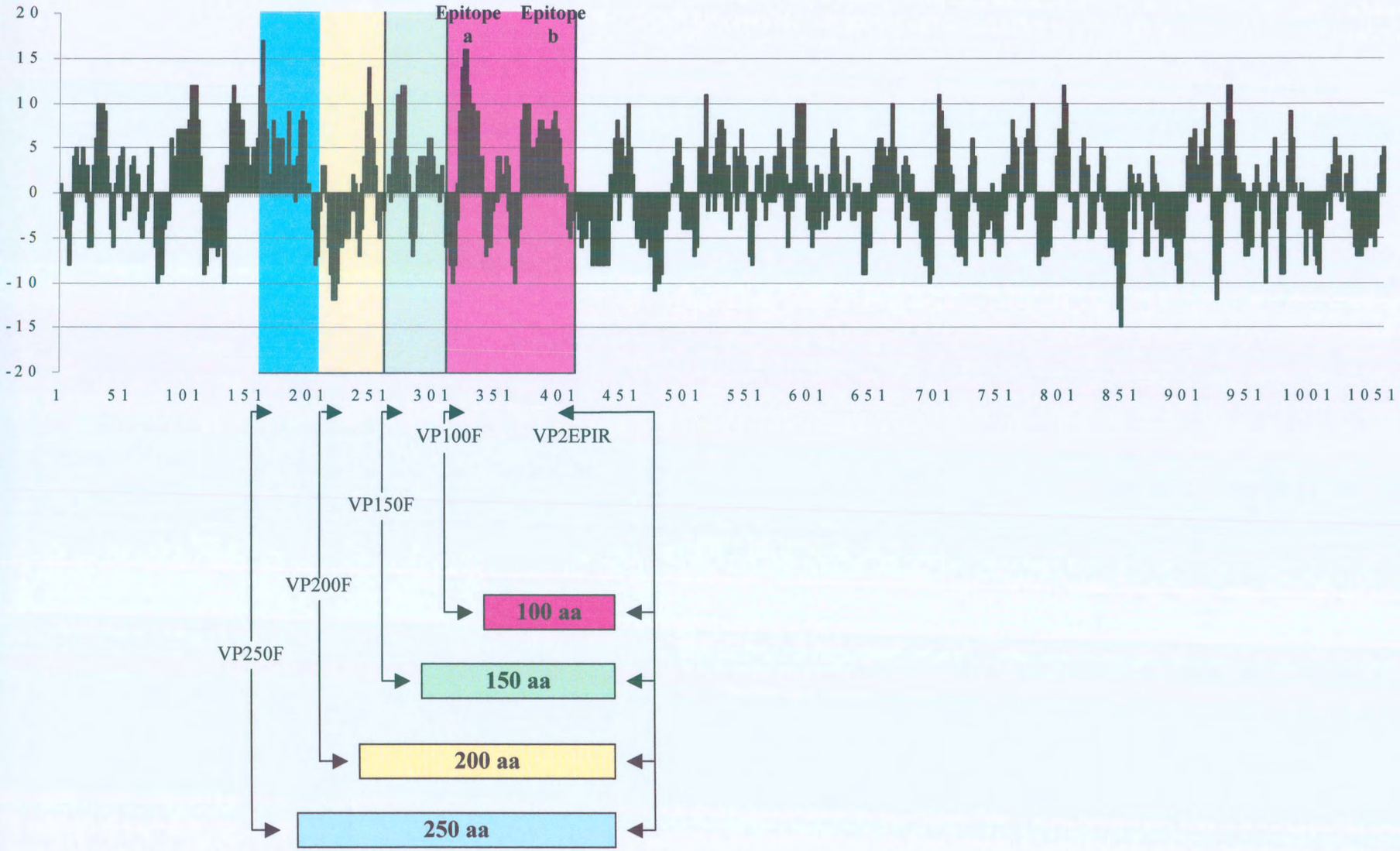

Figure 4.1. Hydrophilicity Plot of AHSV VP2 (Hopp amd Woods, 1981; Hopp and Woods, 1983). Indicated are the PCR primer binding positions and the amplified regions, as well as the positions of the a and b epitopes of VP2.

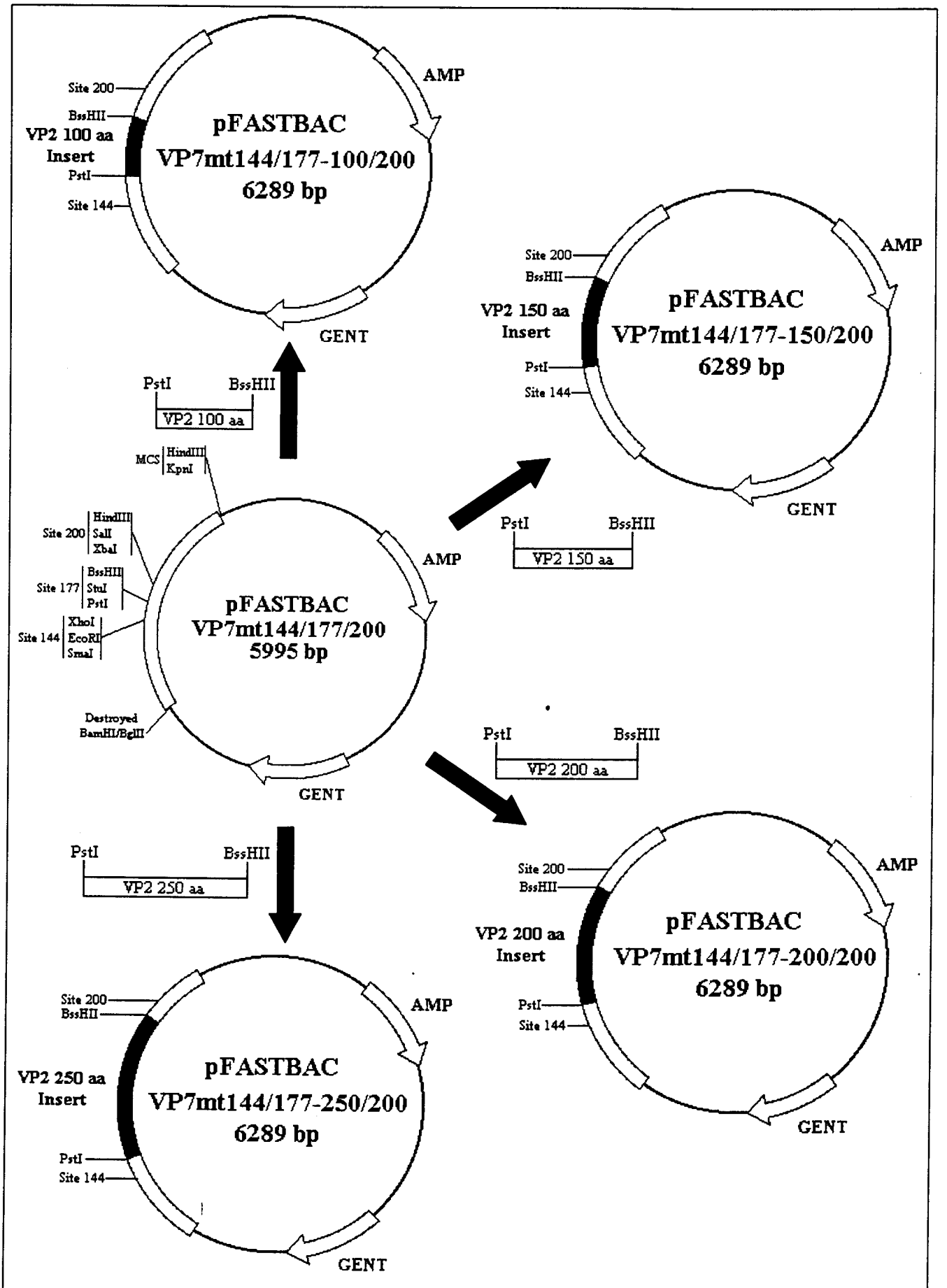

Figure 4.2. Insertion of different size fragments into the 177-site of pFastBac-VP7mt144/177/200

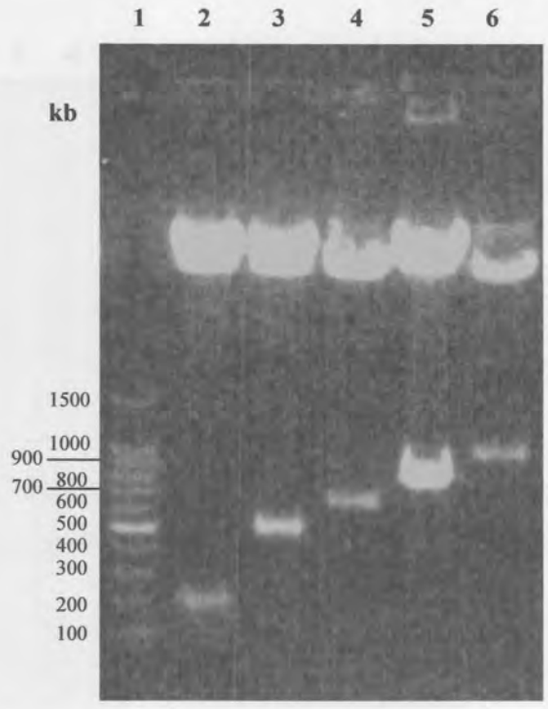

Figure 4.3. 4% Agarose gel electrophoresis of VP7mt144/177/200-insertion mutant digestions. Lane 1 represents the 100 bp DNA Ladder. Lane 2 contains VP7mt144/177/200 digested with *Eco*RI and *Xba*I give rise to linear plasmid DNA and a 204 bp fragment. Lanes 3 to 6 contain VP7mt144/177-100/200, VP7mt144/177-150/200, VP7mt144/177-200/200 and VP7mt144/177-250/200, respectively, digested with *Eco*RI and *Xba*I, which resulted in linear plasmid DNA and 498 bp, 648 bp, 798 bp and 948 bp respective size fragments.

4.3.2. Nucleotide Sequence Determination and Hydropathy Predictions

The primers listed in table 2.1. and table 4.1. were used during automated DNA sequencing (section 2.2.10) to determine the nucleotide sequence of the newly constructed VP7mt144/177-100/200, VP7mt144/177-150/200, VP7mt144/177-200/200, and VP7mt144/177-250/200. Overlapping sequences for each of the four constructs were generated from which the complete gene sequences

could be deduced. In each of the four cases, the sequencing confirmed the presence of the VP2 insert at the 177 position of the VP7mt144/177/200 construct (Appendix C).

No new mutations were generated by the PCR reactions during the synthesis of the inserts, except in VP7mt144/177-100/200. At nucleotide position 557, a guanidine was changed to a thymidine. This was due to a mistake that was made in the VP100F primer because of a faulty template sequence. The substitution resulted in a subsequent change in amino acid 186 from a cysteine to a phenylalanine. This creates a drop in hydrophilicity at that amino acid position from -1.0 to -2.5. This appears to be a rather insignificant change as compared to the hundred foreign amino acids, each with its own charge, that have been inserted into the VP7mt144/177/200 construct.

ClustalX version 1.81 (Higgins and Sharp, 1988; Higgins *et al.*, 1996) was used to do the sequence comparisons and alignments (Appendix C.). Subsequent hydropathy analyses were done (Fig. 4.4.) using the Hopp and Woods predictive method (Hopp and Woods, 1981; Hopp and Woods, 1983) from the ANTHEPROT package (Geourjon *et al.*, 1991; Geourjon and Deleage, 1995).

Table 4.2. Hydrophilic character AHSV-4 VP2 amplified regions (Hopp and Woods, 1981; Hopp and Woods, 1983).

Insert	Hydrophilic Character of Insert	
	Total	**Average**
VP2 100 aa	+228	+2.28
VP2 150 aa	+366	+2.44
VP2 200 aa	+279	+1.395
VP2 250 aa	+425	+1.7

Each of the inserts has a unique overall hydrophilic character, as shown in Table 3.2. All four of the inserts are overall hydrophilic in nature. The degree of hydrophilicity increases with the size of the insert with the exception of the 200 aa insert which is less hydrophilic than the 150 aa insert. This is due to the fact that the 200 aa insert has a large number of hydrophobic regions in the last 50 aa (Appendix C-4), which lowers the average hydrophilic character for the 200 aa and 250 aa inserts. The hydrophilic domains of the inserts are presumed to contain a number of the neutralising epitopes of AHSV VP2 serotype 4.

(a) **VP7mt144/177-100/200 Hydrophilicity Plot**

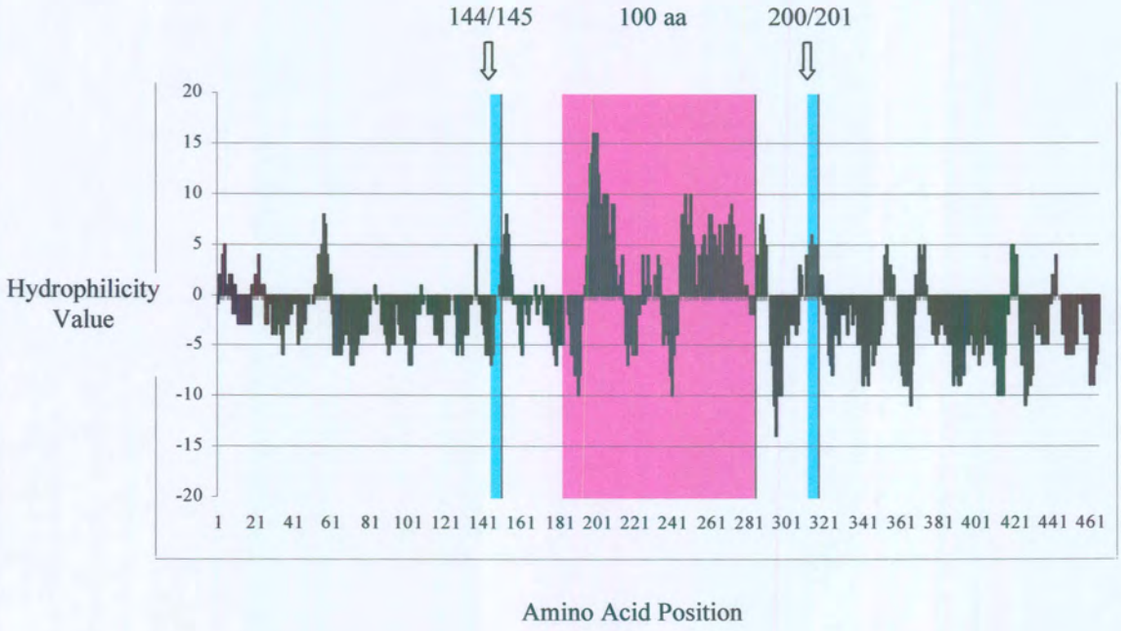

(b) **VP7mt144/177-150/200 Hydrophilicity Plot**

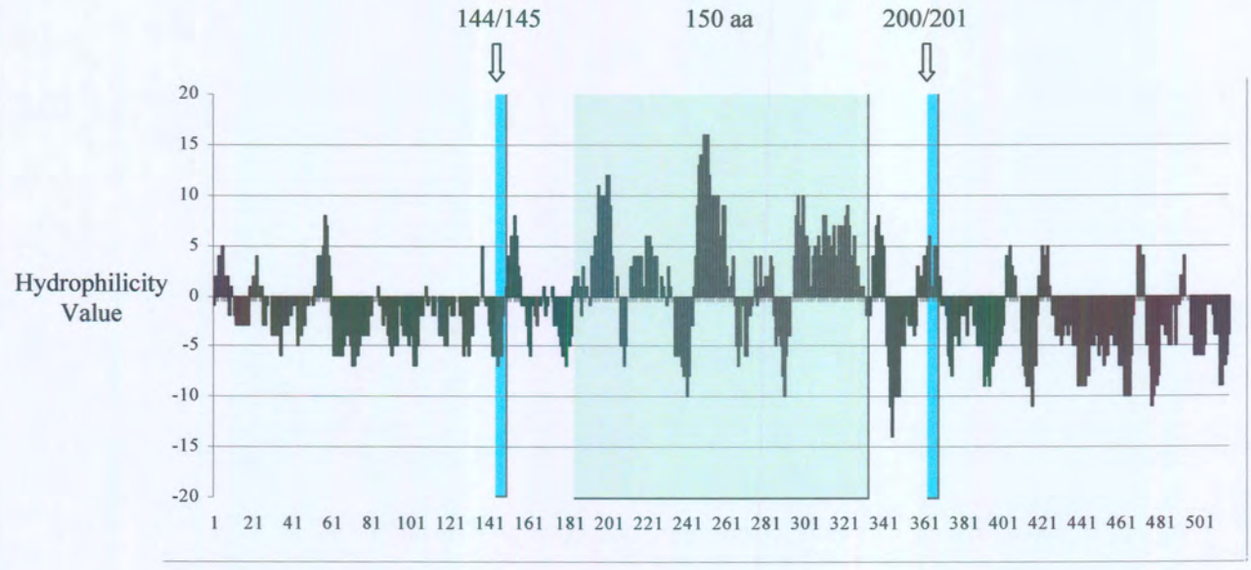

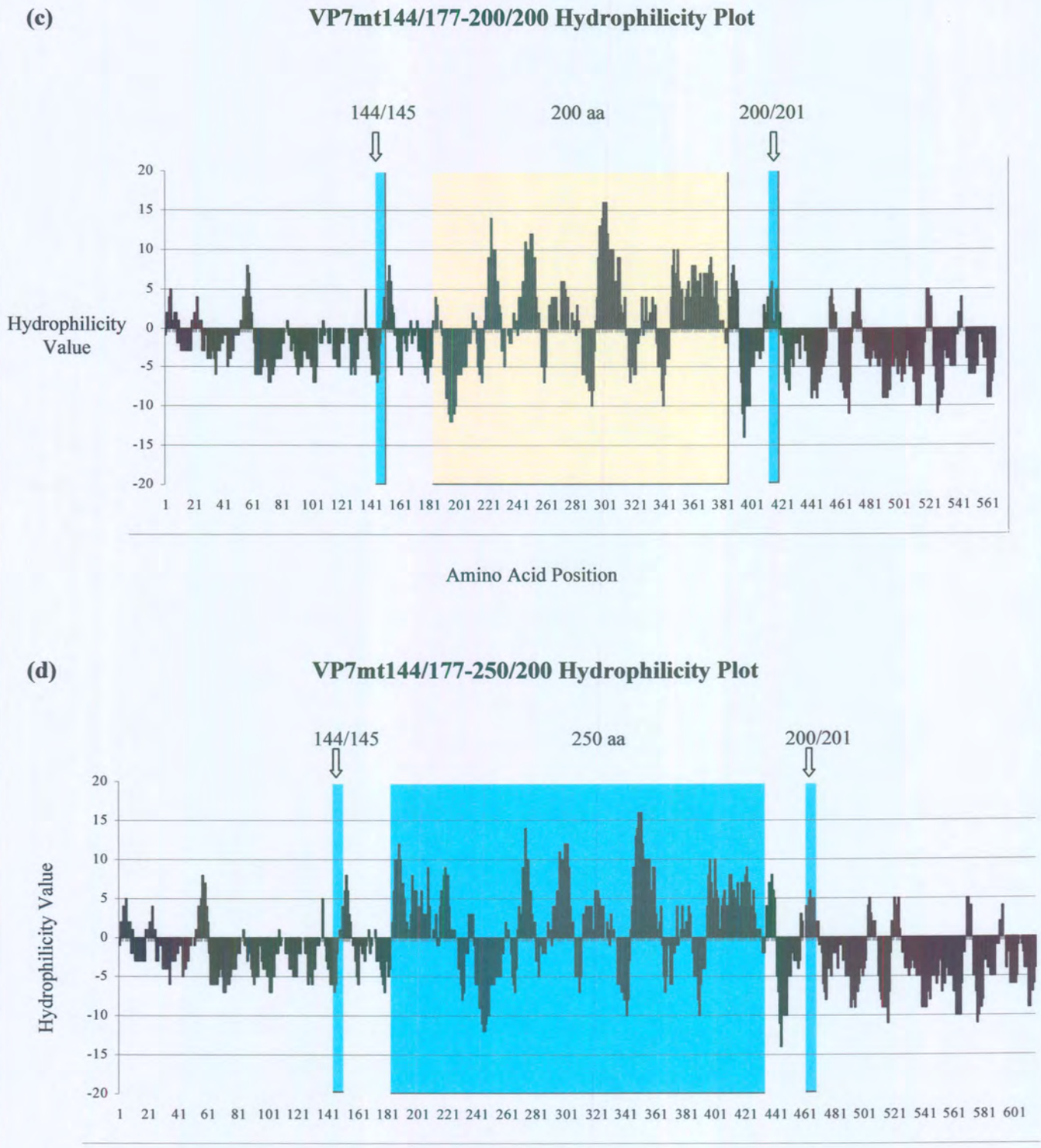

Figure 4.4. Hydrophilicity Plots of (a) VP7mt144/177-100/200, (b) VP7mt144/177-150/200, (c) VP7mt144/177-200/200 and (d) VP7mt144/177-250/200 according to the Hopp and Woods Predictive method (Hopp and Woods, 1981; Hopp and Woods, 1983).

4.3.3. Baculovirus Expression

The four constructs were expressed using the Bac-to-Bac™ expression system. The pFastBac transfer vectors containing the recombinant constructs were transformed in the *E.coli* DH_{10}Bac™ cells, which contain the baculovirus genome. Transposition of the mutant VP7-VP2 genes occurred into the baculovirus genomes (2.2.13), which were later selected for and isolated (2.2.14). Sf9 insect cells were transfected with the recombinant bacmid DNA (2.2.15) followed by infections with the newly generated recombinant baculoviruses.

SDS-PAGE gel electrophoresis (2.2.17) was used to verify protein expression. The gel analysis (Fig. 3.5.) clearly indicates the expression of VP7mt144/177-100/200 (50 kDa), VP7mt144/177-150/200 (56 kDa), VP7mt144/177-200/200 (62 kDa) and VP7mt144/177-250/200 (68 kDa). Although there is a marked decrease in protein expression of the four new recombinant proteins are compared to the expression levels attained by VP7mt144/177/200, the VP7 recombinants are nevertheless still expressed in relatively large amounts. It seems as if the recombinant with the 250 aa insert is expressed better than the three other recombinants, although this might only be an isolated incidence.

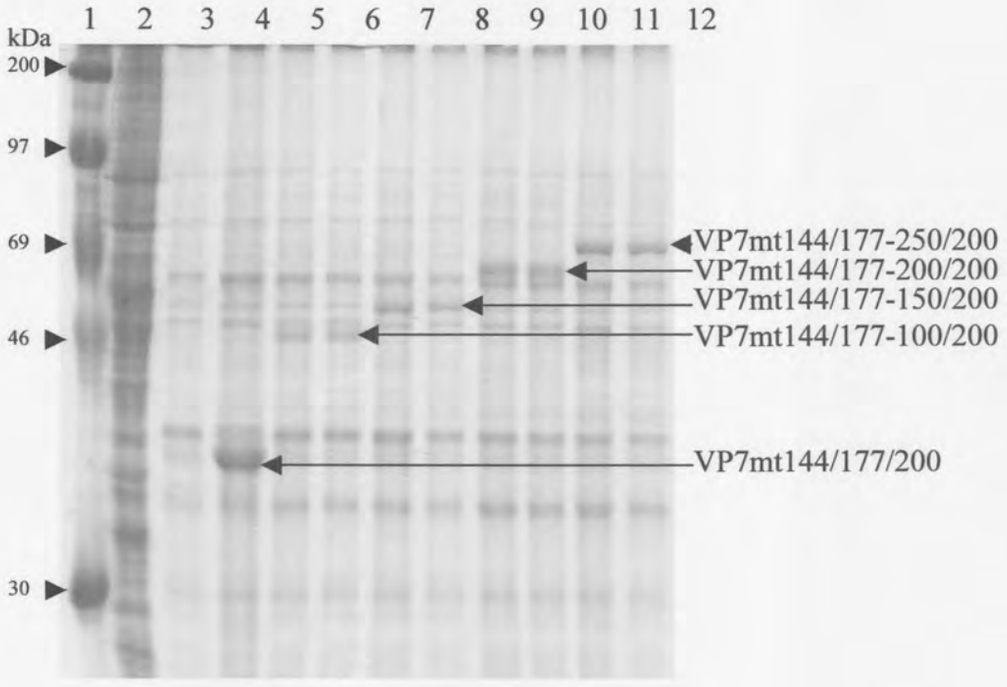

Figure 4.5. A 15% SDS-PAGE analysis of VP7mt144/177/200-insertion mutants' expression. Lane 1 represents the protein size marker. Lane 2 and 3 contain proteins from a mock infection and wild-type baculovirus-infected cells respectively. Lane 4 contains expressed VP7mt144/177/200 (39 kDa). Lanes 5 and 6 contain the 50 kDa VP7mt144/177-100/200 protein, whereas lanes 7 and 8 contain the 56 kDa VP7mt144/177-150/200 protein. Lanes 9 and 10 contain the VP7mt144/177-200/200 protein (62 kDa) and, cell lysates of cells infected with the VP7mt144/177-250/200 construct (68 kDa), are shown in lanes 11 and 12.

4.3.4. Purification of VP7 Particles on Sucrose Gradients

Sucrose gradient analysis was carried out to investigate whether the insertions that have been made, affected the formation, sedimentation and purification of the structure formed by the modified VP7mt144/177/200 mutant. Sf9 cells were infected with the recombinant baculoviruses expressing the VP7mt144/177-100/200, VP7mt144/177-150/200, VP7mt144/177-200/200 and VP7mt144/177-250/200 constructs. The proteins were harvested after 72 h by cell lysis and purification by rate zonal centrifugation on a 50%-70% discontinuous sucrose gradient. The Sigma Gel™ software program (Jandel Scientific) was again used to measure and quantify each fraction's relative protein band intensity on the SDS-PAGE gels. The experiments were repeated several times to exclude inherent possibilities of variation.

The solubility studies of the four recombinant constructs were all compared to that of VP7mt144/177/200. Further comparisons were done by sonication of the pellets of the four constructs after sucrose gradient analyses. These sonication studies were carried out to disrupt the large aggregates in the pellet and to determine if different constructs differed with respect to sonication, reflecting differences in stability. Figure 4.6. shows the comparative protein distribution of VP7mt144/177-100/200. The unsonicated protein distribution resembles the distribution formed by the VP7mt144/177/200 construct. The aggregated percentage proteins in the pellet are approximately the same although the distribution of VP7mt144/177-100/200's proteins in the first five fractions is considerably lower. VP7mt144/177/200, however, has a much lower percentage of small particles in the last three fractions of the gradient than VP7mt144/177-100/200. Whereas VP7mt144/177/200 almost forms no small particles, VP7mt144/177-100/200 has approximately 22% of these protein structures. These small particles could possibly be free soluble trimers. This could point to instability caused by the insertion, with a shift from large particulate structures to smaller, perhaps trimeric, structures.

The sucrose gradient sedimentation profile of VP7mt144/177-150/200 differs from that of VP7mt144/177/200 (Fig. 4.7.). Approximately only half of the VP7mt144/177-150/200 proteins occur in the sucrose gradient pellet, when compared to VP7mt144/177/200, which indicates a decline in aggregation between the particulate structures. Most of the VP7mt144/177-150/200 proteins occur in the first four fractions of the sucrose gradient with approximately 17% in the last three soluble fractions. This same protein fractional distribution as displayed by VP7mt144/177-150/200 is followed by VP7mt144/177-250/200 (Fig. 4.9.).

Figure 4.8. shows the protein distribution of VP7mt144/177-200/200 compared to VP7mt144/177/200. It was found that 85% of the VP7mt144/177-200/200 protein is present in the aggregated structures found in the pellet of the gradient, compared to only 56% for VP7mt144/177/200. It is also seen that only about 8% of VP7mt144/177-200/200 occur in the last three fractions as smaller particles and only 6% in the first three fraction of the gradient. This elevated aggregation is probably caused by the elevated hydrophobicity of the insertion.

VP7mt144/177-200/200 and VP7mt144/177-150/200 have similar protein fractionation profiles after sonication. These profiles resemble that of VP7mt144/177/200, except that the percentage proteins in the bottom of the gradient are a little less whereas the percentage proteins in the top of the gradient are increased. This increase indicates a greater tendency of these two constructs to form much smaller particle structures. This might be instability caused by the insertions. Whereas the third and fourth fractions of sonicated VP7mt144/177/200 are approximately the same, VP7mt144/177-100/200's third fraction is less than half of its fourth fraction. This is indicative of a slight shift in the particulate size. The rest of the protein particle distribution attained by VP7mt144/177-100/200 follow the same particle distribution as that of VP7mt144/177-150/200 and VP7mt144/177-200/200. Sonicated VP7mt144/177-250/200 also shares this protein distribution except for a peak in the first and eighth fractions. It is the eighth fraction that is most notable, reaching a peak with approximately triple the percentage proteins than any of the other constructs. A definite preference for smaller particulate structures is shown by the VP7mt144/177-250/200 construct, although larger particulate structures are still possible.

4.3.6. Scanning Electron Microscopy (S.E.M.)

Protein samples for S.E.M. studies were collected from the second, third and fourth fractions. These pooled fractions were then fixed, mounted and spatter coated with gold-beladium particles. The structures formed by the all four of the new constructs (Fig 4.10) resemble the structures formed by the VP7mt144/177/200 proteins (Fig 2.13.c and d). Most of the structures have the same 8 μm rough, flat and almost circular appearance and share the same surface texture. When high concentration of the proteins are mounted, aggregation, in the form of web-like tentacles/ cables, can be observed between the units.

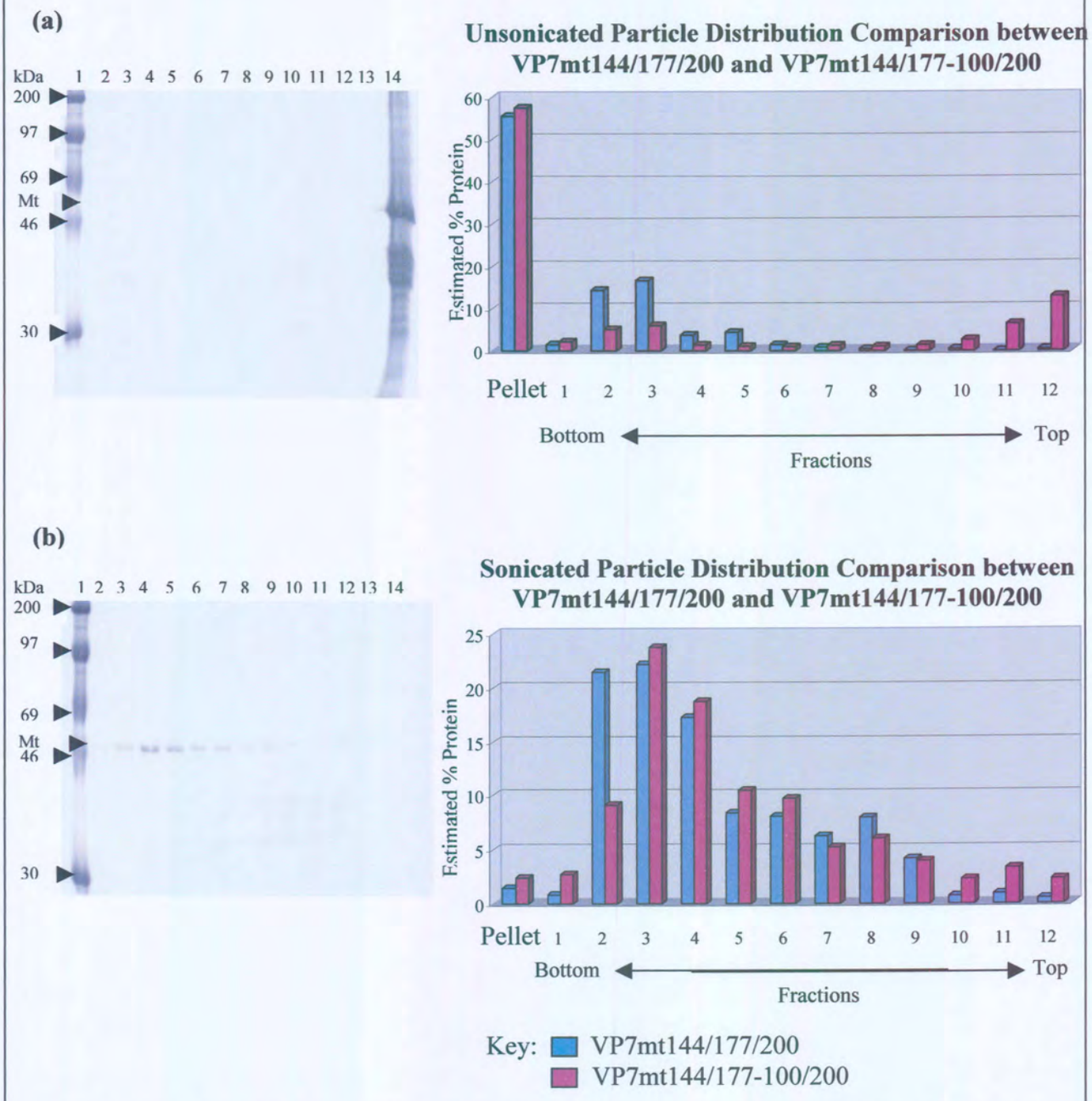

Figure 4.6. Comparative protein distribution between (a) unsonicated VP7mt144/177/200 and VP7mt144/177-100/200. (b) Represents a comparative protein distribution between 25 pulse sonicated pellets of VP7mt144/177/200 and VP7mt144/177-100/200. Proteins were centrifuged on a 50%-70% sucrose gradient using a Sorvall AH-650 rotor at 12000 rpm for 75 min at 4°C, analyzed by SDS-PAGE electrophoresis, quantified by the Sigma Gel™ analysis program and converted to the shown graphic form. On the SDS-PAGE gels, lane 1 contains the protein size marker, whereas lanes 2-13 contain the fractions as collected from the bottom to the top of the gradients. Lane 14 represents the protein pellet of the gradient.

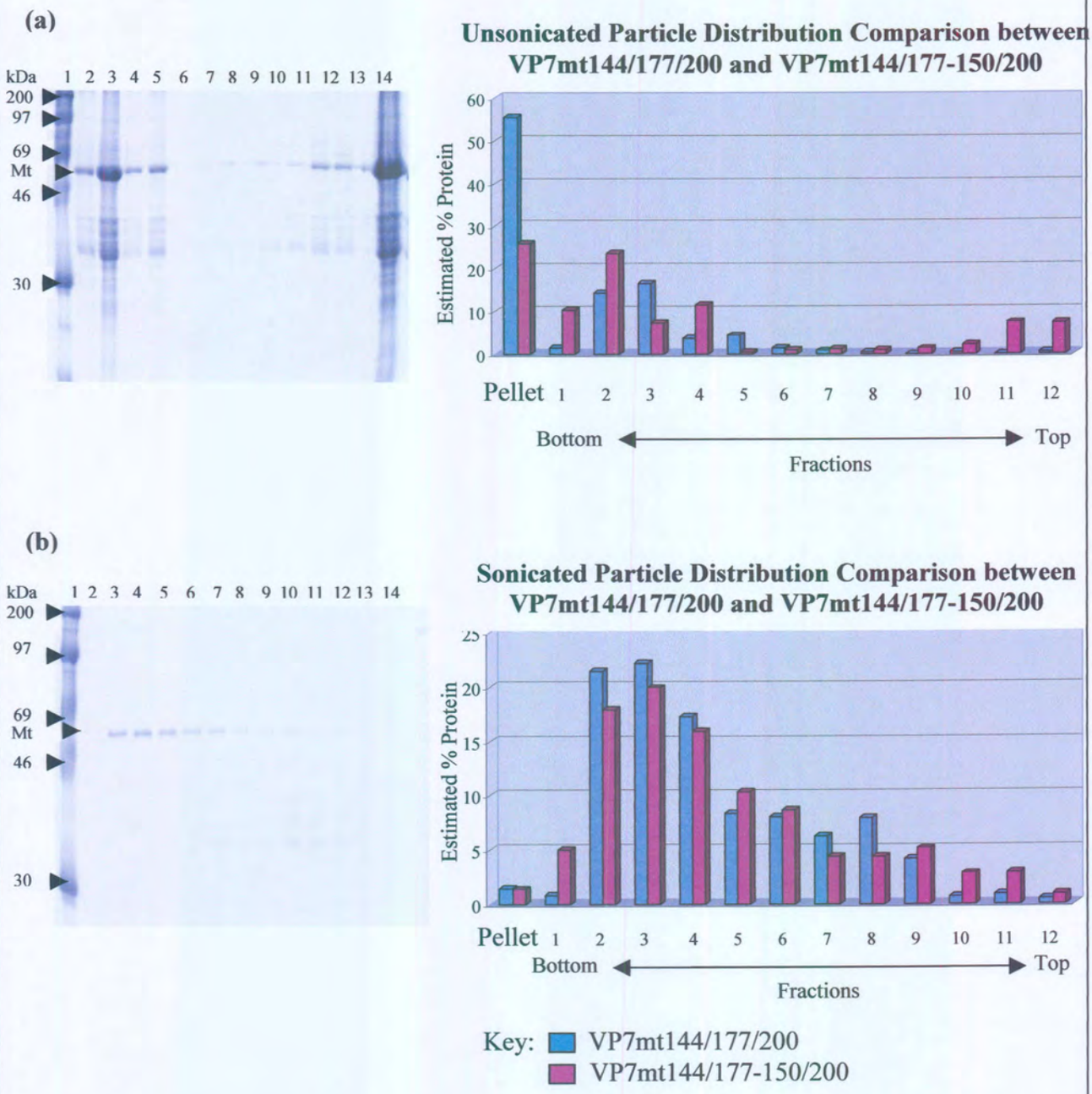

Figure 4.7. Unsonicared (a) and 25 pulse sonicated (b) protein distribution comparison between VP7mt144/177/200 and VP7mt144/177-150/200. Proteins were purified on a 50%-70% sucrose gradient using a Sorvall AH-650 rotor at 12000 rpm for 75 min at 4°C, before analysis by SDS-PAGE electrophoresis. Sigma Gel™ analysis program was used to quantify the protein amounts before conversion to the shown graphic form. On the SDS-PAGE gels, lane 1 contains the protein size marker, whereas lanes 2-13 contain the fractions as collected from the bottom to the top of the gradients. Lane 14 represents the protein pellet of the gradient.

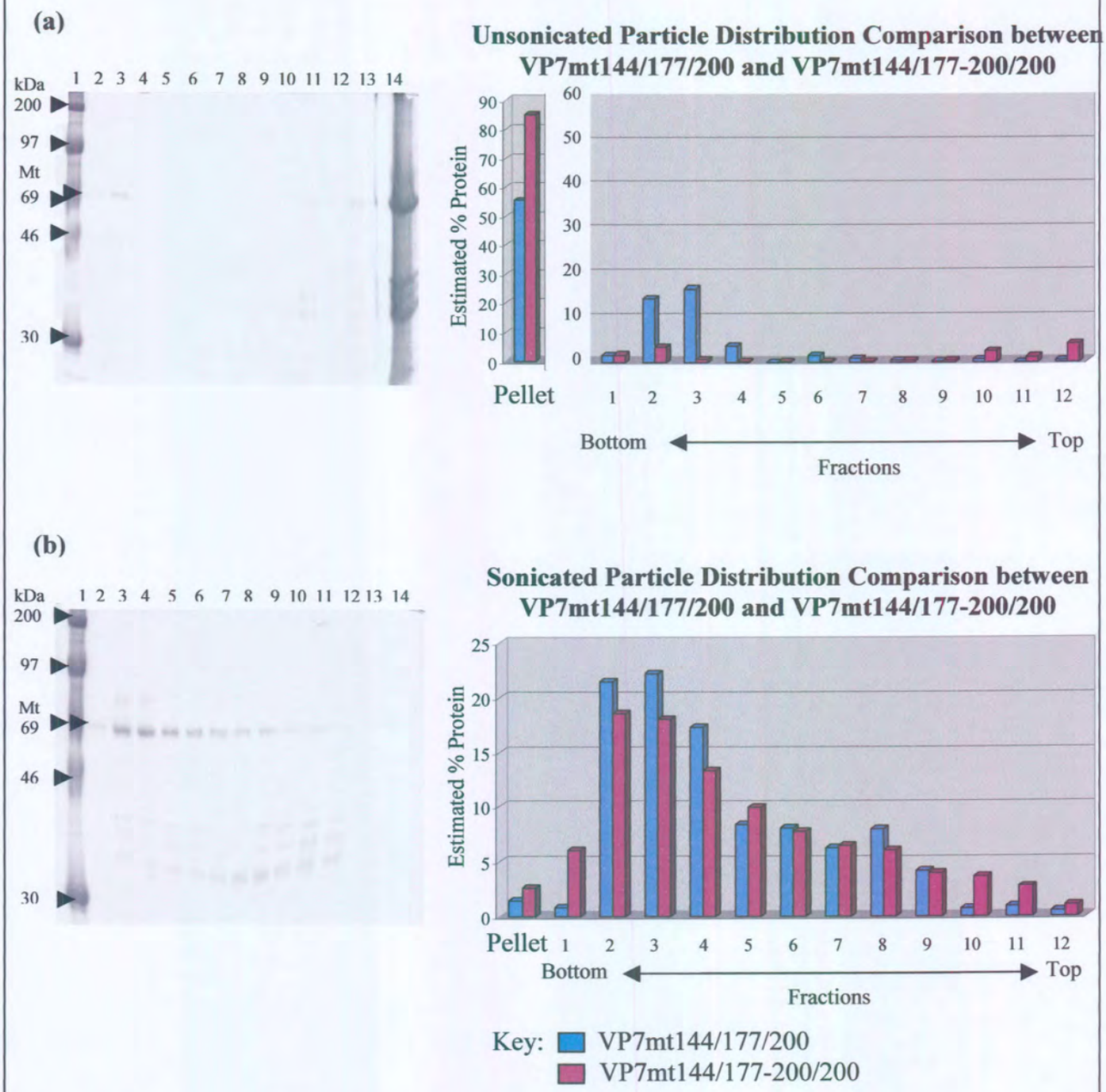

Figure 4.8. (a) Comparison in protein distribution between unsonicated VP7mt144/177/200 and VP7mt144/177-200/200. (b) Comparison in protein distribution between 25 pulse sonicated pellets of VP7mt144/177/200 and VP7mt144/177-200/200. A Sorvall AH-650 rotor was used to centrifuge proteins on a 50%-70% sucrose gradient at 12000 rpm for 75 min at 4°C. Fractions were analyzed by SDS-PAGE electrophoresis, quantified by the Sigma Gel™ analysis program and converted to the shown graphic form. On the SDS-PAGE gels, lane 1 contains the protein size marker, whereas lanes 2-13 contain the fractions as collected from the bottom to the top of the gradients. Lane 14 represents the protein pellet of the gradient.

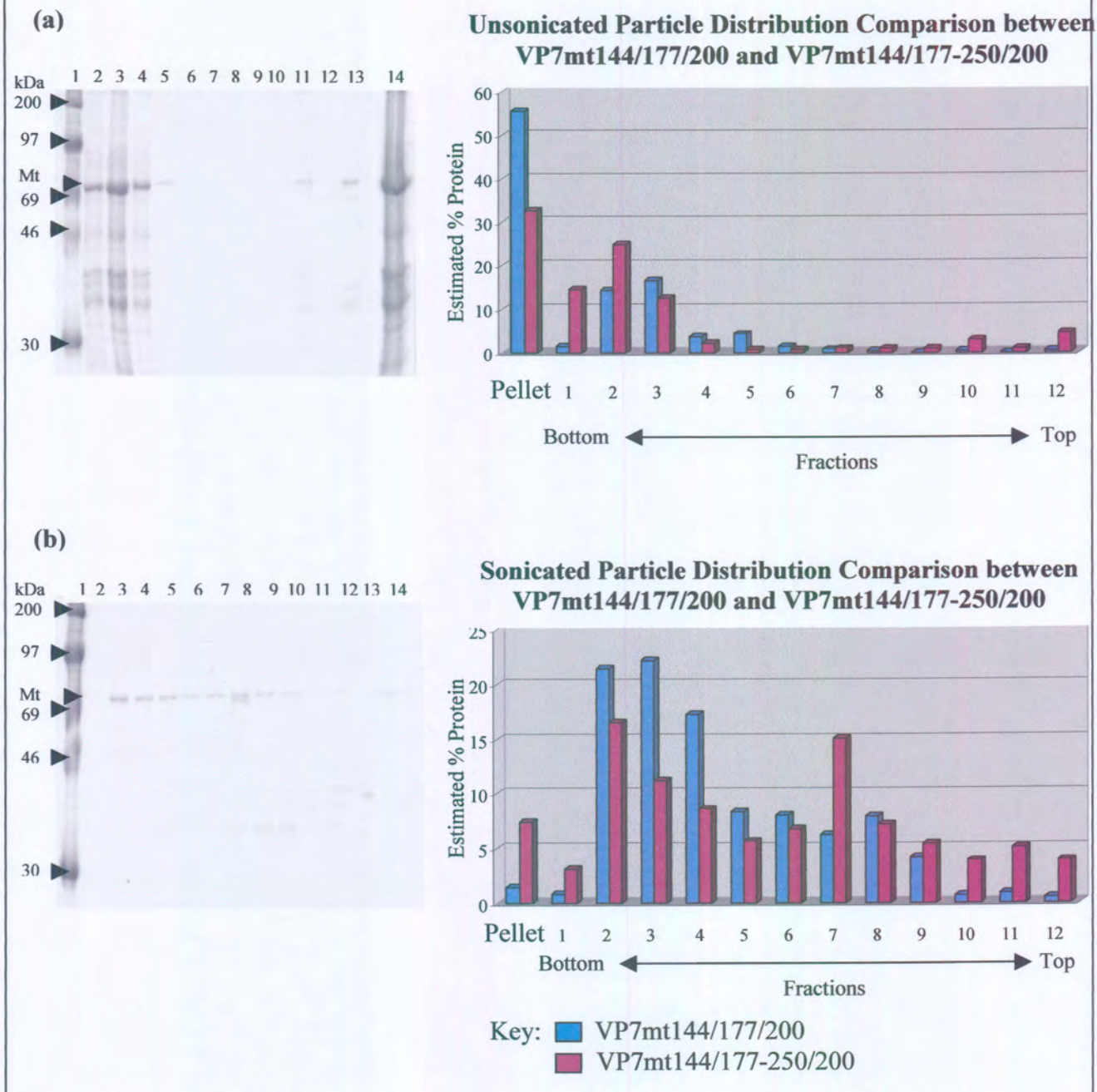

Figure 4.9. (a) Comparison between protein distributions of unsonicated VP7mt144/177/200 and VP7mt144/177-250/200. (b) Represents a comparative protein distribution between a 25 pulse sonicated pellets of VP7mt144/177/200 and VP7mt144/177-250/200. Proteins were centrifuged on a 50%-70% sucrose gradient using a Sorvall AH-650 rotor at 12000 rpm for 75 min at 4°C, analyzed by SDS-PAGE electrophoresis, quantified by the Sigma Gel™ analysis program and converted to the shown graphic form. On the SDS-PAGE gels, lane 1 contains the protein size marker, whereas lanes 2-13 contain the fractions as collected from the bottom to the top of the gradients. Lane 14 represents the protein pellet of the gradient.

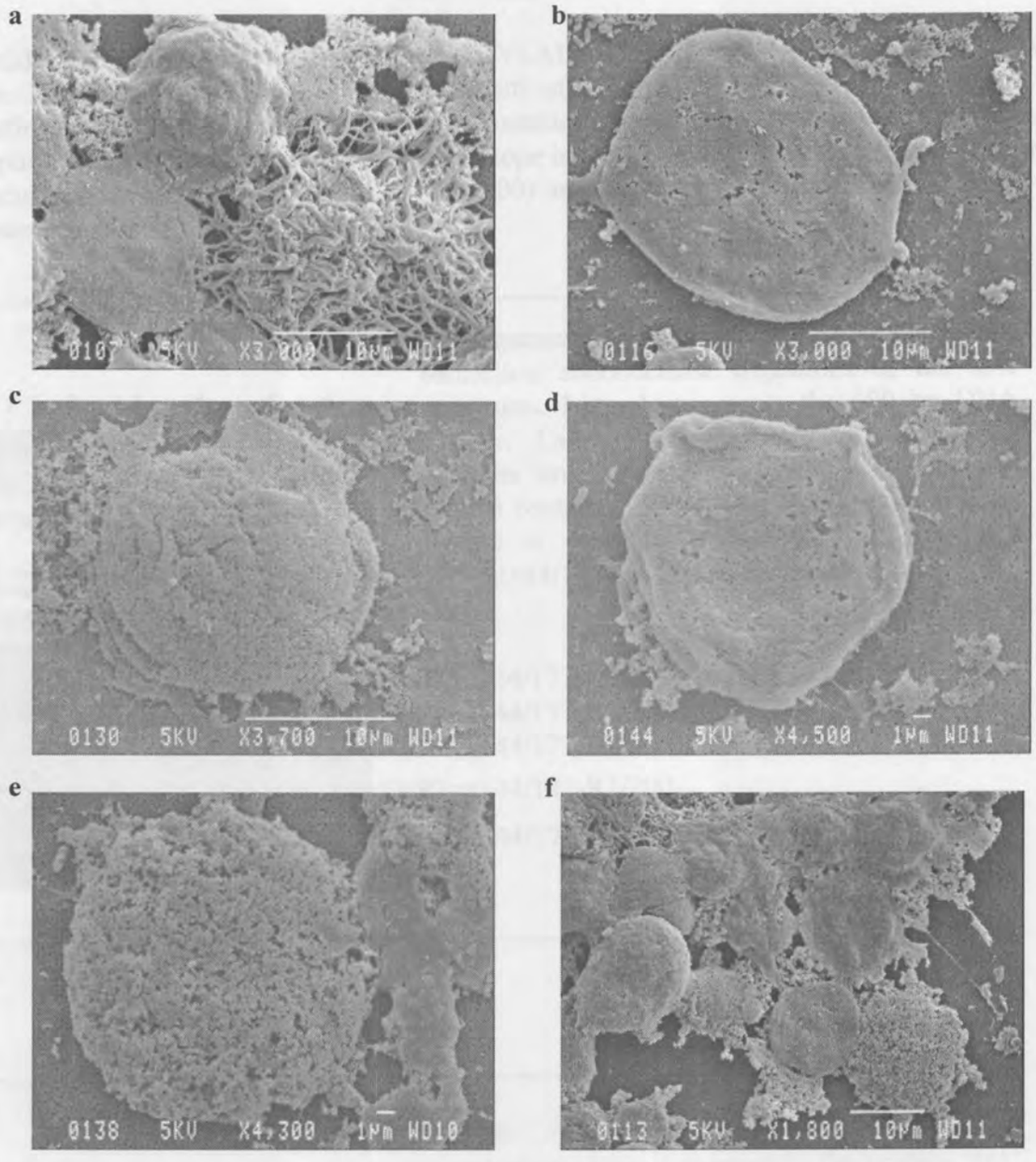

Figure 4.10. Scanning Electron Microscopy photographs depicting the structures formed by the different protein constructs: (a) VP7mt144/177-100/200 (b) VP7mt144/177-150/200, (c) VP7mt144/177-200/200, (d) and (e) VP7mt144/177-250/200. (f) Depicts a wide-angle view of the aggregated structures attained at high concentrations.

4.4. Discussion

One of the greatest challenges to subunit vaccines is the possible size of the inserts that can be made into the subunit protein without causing it to lose structure. The structure must be able to accommodate large epitope-containing insertions to increase the usefulness of the vaccine. The structure should also be able to accommodate insertions with different hydrophilic characteristics. As mentioned in chapter 1, the only licensed subunit vaccine in the United States of America is the hepatitis B virus surface antigen, which assembles into subviral particles similar to that of hepatitis B. The largest insertion that has been made into these particles without the loss of the structure, was 238 amino acids (Beterams *et al.*, 2000). The creation of VP7mt144/177/200 by the insertion of three multiple cloning sites, had an effect on the crystal formation abilities. These insertions did not, however, destroy the protein's trimer formation abilities or the trimers' ability to aggregate in organised structural units similar to the hexagonal crystals formed by wild type VP7.

To test VP7mt144/177/200's ability to function efficiently as a subunit vaccine, large insertion with different hydrophilic characteristics were made. The insertions cloned into the 177 aa site of VP7mt144/177/200 includes a 100 aa, 150 aa, 200 aa and 250 aa regions of AHSV-4 VP2. These changes to VP7mt144/177/200 contributed to the overall hydrophilicity of the protein (Table 4.2), the impact of which could not be determined at the early stages before solubility studies.

The 100 aa insertion into VP7mt144/177/200 to create VP7mt144/177-100/200 added a net hydrophilic character of +228 to the construct. This added hydrophilicity shifted the solubility of the construct, making the construct more soluble; possibly resulting in the increase of smaller particulate structures that was observed. This is supported by the results in figure 4.6.b., where the sonicated fractions containing the largest percentages proteins are fractions three and four for VP7mt144/177-100/200, whereas it is fractions two and three for VP7mt144/177/200. Also observed, was an approximate 22% increase in the percentage in the top of the gradient during the VP7mt144/177-100/200 solubility study (Fig. 4.6.a.).

The insertion of 150 aa domain into VP7mt144/177/200 had a different reaction on the solubility of VP7mt144/177/200 than the 100 aa insertion. The increased hydrophilic character of +366 lowered the aggregation ability of the protein structures. Less than half of the proteins that occur in the pellet of VP7mt144/177/200, is present in the VP7mt144/177-150/200 construct's pellet (Fig. 4.7.a). The rest of the proteins are distributed in the fractions with an increase of 16% small particles at the top of the

gradient, possibly free trimeric structures. The effect of the hydrophilic character is best illustrated by the 200 aa insertion. As mentioned before, the 200 aa amplified region is very hydrophobic in the last 50 aa. This region lowers the hydrophilic character of the insert to a net of +279, which is more than 100 aa insertion but far less than hydrophilic character of the 150 aa insertion. The effect can clearly be seen in figure 4.8.a. where 85% of the VP7mt144/177-200/200 proteins are aggregated in the pellet of the sucrose gradient. Speculations that this might be a result of an increase in size are abandoned when examining the solubility profile of VP7mt144/177-250/200 (Fig. 4.9.). Here, as in the 150 aa insertion, a very hydrophilic addition (+425) was made to the VP7mt144/177/200 construct. The solubility profile of VP7mt144/177-250/200 (Fig. 4.9.a.) is almost the same as the profile of VP7mt144/177-150/200. The only difference is seen when studying the sonication results of the structures. VP7mt144/177-250/200 forms a unique peak in the seventh fraction from the bottom of the sucrose gradient. This indicates that a distinct size structure is attained during sonication of the VP7mt144/177-250/200 aggregated proteins from the pellet and an instability in the larger particles.

The ability of the trimers to associate into large structures was confirmed by scanning electron microscopy. All four of the recombinant constructs formed structures that resembled the structures formed by VP7mt144/177/200. This indicates that the structures formed by VP7mt144/177/200 are able to absorb any structural stress if large aa regions with different hydrophilic characteristics are inserted into the 177 aa site.

Chapter 5

Concluding Remarks

The use of AHSV VP7 as a subunit vaccine has come a long way since the idea's first conception by Wade-Evans *et al.*, 1997. What first attracted attention to this protein was its ability to spontaneously form crystals when expressed in recombinant baculovirus infected cells (Chuma *et al.*, 1992). Large quantities of these crystals can easily be extracted from the cells and purified. Later they were shown to be immunogenic, enough for the generation of protective immune responses (Wade-Evans *et al.*, 1997; Wade-Evans *et al.*, 1998). These and other findings justified further investigation into and possible development of a subunit vaccine system using AHSV VP7.

This study was initiated by the creation of a VP7 construct capable of presenting epitopes at multiple sites on the surface of its structure. Multiple cloning sites were created by the insertion of six extra amino acids at the position 144, 177 and 200. These modifications caused an increase in the solubility of the protein but did, however, not eliminate the modified VP7 protein from forming trimers and assembling into distinct flat particles that can be purified easily on sucrose gradients. Large structures, not too different from the hexagonal crystals observed with wildtype VP7, were observed when the particles were analysed by electron microscopy. Also illustrated by these studies were the effect that aggregation has on the structure of these particles. With the storage studies that were conducted on VP7mt144/177/200, it was found that the increased aggregation of this protein would prove troublesome for any storage technique being applied. Sonication reduced the aggregation but this was only a temporary relief. As found by Wade-Evans *et al.*, 1997, whole crystals primarily elicit a protective cell-mediated T-cell immune response with vaccination. This is probably because the large 6 µm crystals are absorbed into antigen presenting cells by means of phagocytosis, where they are broken down to short peptides and presented on the MHC complex to the immune system. Sonication of the structures before immunisation might prove advantageous since this will reduce the size of the injected particles and could lead to humoral immune response generation in addition to the cell-mediated immunity. The easily attained high yield (approximately 0.043 ng/ cell) and purity of the VP7mt144/177/200 protein contributes greatly to its potential use as a subunit vaccine. The high yield is, of course, dependent on the health of the Sf9 cells being used, the viral stocks and other conditions.

Subsequent structural studies were conducted by inserting epitopes into at least two of the three newly created sites. The effect that the use of different sites has on the structure was best illustrated by the

creation of the VP7mt144/177-A/200 and the VP7mt144-B/177/200 constructs. The insertion of the hydrophilic VP2 'a' epitope into position 177 of VP7mt144/177/200 resulted in an increase in solubility but also an increase in aggregation. This was in contradiction to the results attained by the insertion of the hydrophilic VP2 'b' epitope at amino acid position 144 of VP7mt144/177/200, which also resulted in an increased solubility but a decrease in aggregation. These results were confirmed by the creation of a construct containing both the epitopes at their respective sites, VP7mt144-B/177-A/200. This construct had intermediate aggregational tendencies, the same level as that of the original VP7mt144/177/200 construct. All three constructs seemed to form the same size structures when aggregation was removed by sonication. The formation of particulate structures was confirmed by subsequent electron microscopy studies.

As mentioned, a major disadvantage of virus like particles as antigen carriers, is the limitation of their insertion capacity. Studies were conducted into the size of the possible inserts that can be made into the VP7mt144/177/200 construct without causing it to lose its particulate structure. A maximum of 250 amino acids from VP2 was inserted into VP7mt144/177/200 without an alteration to the particulate structures still being formed. These experiments also illustrated the effect that the hydrophilic characters of the inserts have on the overall structure of VP7mt144/177/200. These size experiments are, however, incomplete and future investigations should include studies into the effect of large insertions into the other two sites on the VP7mt144/177/200 construct. Also, the effect of large amino acid insertions into all three the multiple cloning sites at once.

Other future investigations that should be conducted to further the development and potential of VP7 as a vaccine delivery system, include the following:

- This study lacked investigations into the actual immune response generated by these constructs. These studies would indicate whether or not the inserted epitopes are presented efficiently to the immune system. Also, comparative studies should be done concerning the generated protective immune responses between whole particulate injection and the sonicated product injection.

- Another relevant area of investigation should be conducted on the use of non-polar chemical solvents for dissolving the aggregated proteins before injection.